Ecological Complexity 43 (2020) 100853

Contents lists available at ScienceDirect

Ecological Complexity

journal homepage: www.elsevier.com/locate/ecocom

Aquaculture, pollution and fishery - dynamics of marine industrial interactions

Harald Bergland*[,a], Evgenii Burlakov[b,c], Pål Andreas Pedersen[d], John Wyller[e]

[a] School of Business and Economics, Campus Harstad, University of Tromsø - The Arctic University of Norway, P.O. Box 1063Harstad N-9480, Norway
[b] X-Bio Institute, University of Tyumen, 6 Volodarskogo St., Tyumen 625003, Russia
[c] V.A. Trapeznikov Institute of Control Sciences of Russian Academy of Sciences, 65 Profsoyuznaya St., Moscow 117997, Russia
[d] Nord University Business School, P.O. Box 1490, Bodø N-8049, Norway
[e] Faculty of Science and Technology, Norwegian University of Life Sciences, P.O. Box 5003, Ås N-1432, Norway

ARTICLE INFO

Keywords:
Aquaculture
Fishery dynamics
Equilibrium states,

ABSTRACT

We model bioeconomic interrelations between a commercial fishery and an aquaculture industry by using a dynamical systems theory approach. The biomass follows a logistic growth where the pollution emerging from aquaculture is accounted for by means of a retardation term. We investigate the existence and stability of the equilibrium states of this model as a function of the growth-retardation parameter and find that a necessary (but not sufficient) condition for stability is low and moderate values of the emission-remediation ratio. Three intervals of the growth-retardation parameter are identified in this regime of the emission-remediation ratio. The regime of low and negligible influence of the pollution on the biomass evolution gives rise to the existence of an asymptotically stable equilibrium state characterized by a finite biomass and a finite effort in the fishery. In the same regime we identify two unstable equilibrium states of which the former one is characterized by no effort in the fishery, whereas the latter one is characterized by no biomass and no effort. When the growth retardation parameter exceeds a certain threshold, the fishery becomes unprofitable and the equilibrium state characterized by no effort in the fishery becomes asymptotically stable. By a further increase in this parameter above a higher threshold value, also the biomass is wiped out and the equilibrium state characterized by no biomass and no effort becomes asymptotically stable.

1. Introduction

In recent years politicians and marine researchers have become increasingly engaged in the socalled *blue economy*. In the blue economy one considers all human activities taking place in coastal areas and the ocean. This notion also includes business activities that could possibly harm the biological life and cause externalities that may reduce other possible uses of the oceans' natural resources. A sustainable blue economy implies a focus on the possible effects of increasing sea farming on the environment in general, and in particular the effect this industry has on wild fish harvesting, given that the fisheries are managed in a sustainable way. The notions of blue economy and blue growth are defined and debated by Kathijotes (2013), Silver et al. (2015), Smith-Godfrey (2016), Spalding (2016) and Golden et al. (2017).

In the present paper we propose a conceptual dynamical model consisting of a single species commercial fishery, an aquaculture industry, and bioeconomic interrelations between these industries. Both the harvesting sector and the aquaculture production sector are supposed to consist of many small production units, with the product prices as given in the consumption markets. However, the total supply from these industries determines the value of farmed and wild fish in the market. Additionally, the aquaculture industry produces emissions that may harm the reproduction ability and/or growth potential in wild fish stock.

Aquaculture production may have significant negative effects on the aquatic environment, as discusses by Dempster et al. (2009), Lorenzen et al. (2012), Liu et al. (2014), Christensen (2017), Svåsand et al. (2016) and Grefsrud et al. (2018). Aquaculture plants also leads to a physical occupation of ocean areas that may negatively affect the productivity in harvesting. See Hoagland et al. (2003), Mikkelsen (2007), and Foley et al. (2012).[1] The possible negative externalities from aquaculture often result in governmental regulations, such as capacity constraints on the volume of farmed fish, area restrictions, etc. (Hersoug, 2012; NFD, 2014). The possible conflicting interests between commercial harvesting and

* Corresponding author.
E-mail address: harald.bergland@uit.no (H. Bergland).

[1] The problem of more areas allocated for aquaculture is also discussed in Bergland et al. (2018).

https://doi.org/10.1016/j.ecocom.2020.100853
Received 17 December 2019; Received in revised form 28 May 2020; Accepted 2 July 2020
Available online 10 July 2020

aquaculture are described and analyzed by Hoagland et al. (2003), Hannesson (2003), Mikkelsen (2007), Jiang (2010), Regnier and Schubert (2016) and Bergland et al. (2018).

We consider activities in aquaculture that cause a release of nutrients, particles and fish waste, in addition to undesirable chemical substances from medicine use or other inputs in aquaculture production. The environment has some absorptive capacity regarding this pollution. The degradation rate of the pollution depends on the pollutant density. As long as the emission rate does not exceed nature's own absorptive capacity, wastes may not accumulate (Watson et al., 2016). We assume that the flow of emissions from the fish farming affects the ability of the marine environment to remediate the waste substances. This mechanism was first described by Haavelmo (1971) and later on discussed in Flaaten (2018). The description of this mechanism was incorporated in a general marine pollution model by Bergland et al. (2019). Furthermore, accumulated pollution from aquaculture production may cause harm on the biological growth in the wild fish stock. Several possible direct and indirect ecosystem mechanisms motivate this assumption. The releases from aquaculture may affect migration, spawning behavior and spawning quality of the wild fish species. As reported in Svåsand et al. (2016), such impacts are uncertain and evidence is limited, but these effects cannot be excluded. Diseases and treatment of diseases in aquaculture may also cause ecosystem disturbances. Undesirable substances from medicine may harm the considered fish stock directly, or harm resources which the commercial species feed on. Possible environmental impacts of chemical use in aquaculture are summarized in Burridge et al. (2010). The importance of this growth-retardation mechanism is characterized by great uncertainty, see Svåsand et al. (2016) and Grefsrud et al. (2018) for more details. The real world uncertainty regarding the strength of this mechanism is a reason to elaborate on the role of the biomass growth-retardation impact in the model. Hence, we consider possible negative ecological externality from aquaculture production on a commercial fishery, and term this the biomass growth-retardation impact from pollution.

Furthermore, we consider the market interrelations between these industries. There are many studies modelling market interactions through price mechanisms in fish product markets, see e.g. the models proposed by Hannesson (1983), Anderson (1985), Hannesson (2003), Regnier and Schubert (2016) and Steinshamn (2017). Following this tradition, we assume that the markets for these two marine products are inter-related in the demand. More farmed fish coming into the market means that the consumers are less willing to pay for an extra unit of farmed fish. Similarly, more harvested fish, leads to less willingness to pay for an extra unit of wild fish. Additionally, when there is an increase in the amount of wild fish into the market, the consumers are willing to pay less for a farmed fish unit. Similarly, when the amount of farmed fish increases, the willingness to pay for harvested fish decreases. Hence, the fish products are presumed to be substitutes in demand. We omit interrelations in the input market, and assume constant unit prices of effort.[2]

Based on this model, we examine biological and economic conditions for the existence of equilibrium states and investigate the stability properties of these states. Our main concern is the biomass growth-weaken impact. We elaborate on how various strength of this negative ecological externality influences the commercial fishery. In particular, we study the consequences on the existence of equilibria and the stability of these equilibria in the model when the biomass growth-retardation effect changes from being negligible to become significant.

The paper is organized in the following way: In Section 2 we describe the principles underlying our modeling framework. This framework is expressed in terms of a 4D autonomous dynamical system. In Section 3 this system is analyzed. We first transform the model to a nondimensional form. Thereafter we summarize the properties of the model with respect to existence and the stability of equilibrium points. We also explore in detail some special cases of our model such as the case with constant product prices and the case with separate price formation. Section 4 contains concluding remarks, and an outlook listing topics for future research. Appendix A–Appendix F contain the detailed mathematical analysis of the model: In Appendix A we prove that the dynamical system under consideration possesses the invariance property. In Appendix B–Appendix E we show the detailed analysis of the existence and stability of the equilibrium points. Appendix F contains a summary of a necessary and sufficient condition for the location of all the zeros of a quartic polynomial in the left half plane, i.e. the Routh-Hurwitz criterion.

2. Model

We consider two industries interacting in the product markets: The aquaculture industry (a) and the wild fishery (f). For the variables and parameters introduced in the Section 2.1, the subscripts a and f refer to these two marine industries. In addition to the market interdependency there are possible externalities from the aquaculture activity influencing the fishery.

2.1. Industry production and externalities

Regarding the aquaculture industry, we assume that the production volume, Y, is modelled as a monotonically increasing power function in the effort allocated to aquaculture, E_a, i.e., as

$$Y = rE_a^k, \quad r > 0, \quad 0 < k < 1. \tag{1}$$

Here r is an exogenous efficiency parameter. The industry may increase its production by inserting more effort. The condition $0 < k < 1$ means a decreasing economy of scale in the sea farming industry, and is common in aquaculture analysis. See Jiang (2010) and Regnier and Schubert (2016). Furthermore, in order to simplify the discussion of the model, we assume the specific scale elasticity value k is given as $k = \frac{1}{2}$.

Let Z denote the time dependent flow of pollution. This represents the harmful residual emissions from the aquaculture production, i.e. waste from feeding, medical treatment etc. The pollution from the aquaculture production can be either a function of the production volume or its use of certain inputs. Here we will use the commonly assumed simplification that this flow of pollution is proportional to the production volume Y, i.e.,

$$Z = \varrho Y, \quad \varrho \geq 0. \tag{2}$$

The positive proportionality constant ϱ is referred to as the *emission parameter*. In addition to the waste flow, we consider accumulation of waste over time as the main environmental problem. We study the pollution problem as a renewable natural resource problem, and assume that the environment has some absorptive capacity. We will describe this process in the following way: For low and moderate values of the pollutant density S, the degradation rate of the pollution will increase with S. When the pollutant exceeds a certain threshold, the ability of the marine environment to carry out self cleaning will be reduced. For high pollutant concentrations, it is negligible. This hypothesis was originally proposed by Haavelmo (1971). In the present work we model this self cleaning ability by means of a positive two times continuously differentiable function g of S, termed the *remediation capacity*. More details about the property of the remediation function can be found in Bergland et al. (2019).

We thus end up with the aquaculture - pollution equation

$$\frac{dS}{dt} = \varrho Y - \rho g(S), \quad \rho > 0. \tag{3}$$

for the pollutant density S when making use of (2). The positive

[2] The consequences of effort market competition are analyzed in Bergland et al. (2018).

proportionality constant ρ is referred to as the *remediation rate*. Furthermore, we specify the remediation capacity by

$$g(S; d) = \frac{S}{S^2 + d^2}, \quad d > 0. \tag{4}$$

This means that we assume that there is no remediation if there are no pollutants present. The parameter d is the pollution density level maximizing the remediation capacity.

We next consider the fish harvesting sector, where the fish supply from harvesting is given by the Gordon-Schaefer production function (Gordon, 1954; Schaefer, 1954)

$$H = qXE_f, \quad q > 0. \tag{5}$$

Here H is the time-dependent supply of fish in the market (harvesting rate), X is the time-dependent fish stock (biomass), E_f is the time-dependent harvest effort and q is a constant harvest efficiency rate.

We combine the production function (5) with a logistic growth model. A modified logistic growth equation for the wild fish specie can be formulated as

$$\frac{dX}{dt} = \sigma X\left(1 - \frac{\alpha S}{K} - \frac{X}{K}\right) - H. \tag{6}$$

Here σ is the intrinsic logistic growth rate and K is the carrying capacity. The term $\frac{\alpha S}{K}$ in (6) represents a decrease in the growth of wild fish due to the presence of the pollution from the aquaculture activity. We assume that $\alpha \geq 0$. The constant α will be referred to as the *growth-retardation parameter*.

Combining (1), (3), (5) and (6), we thus end up with the system

$$\frac{dX}{dt} = \sigma X\left(1 - \frac{X + \alpha S}{K}\right) - qXE_f, \tag{7}$$

$$\frac{dS}{dt} = \varsigma r E_a^{\frac{1}{2}} - \rho g(S; d) \tag{8}$$

for the biomass - pollution part of the model.

2.2. Market and industry profit

We assume that the demand side of the aquaculture market and the wild fishery market are interrelated in the sense that wild fish and farmed fish are substitutes in demand, see for instance Gravelle and Rees (2004). The two products meets the same needs of consumers but are not perfect substitutes. This means that an increase in the price on aquaculture products leads to less demand for farmed fish and more demand for wild fish. Analogously, a higher price on wild fish implies a lower demand for wild fish and a higher demand for aquaculture products. These characteristics of the demand side can be described and specified by the price functions

$$P_a(Y, H) = A_a - \beta_a B_a \frac{Y}{Y + B_a} - \beta_{af} D_a \frac{H}{H + D_a}, \tag{9}$$

$$P_f(H, Y) = A_f - \beta_f B_f \frac{H}{H + B_f} - \beta_{fa} D_f \frac{Y}{Y + D_f}. \tag{10}$$

where P_a and P_f measures the prices on aquaculture products and wild fish respectively. The chosen specification of the demand functions has some characteristics:

$$A_i > 0, \quad B_i \geq 0, \quad D_i \geq 0, \quad \beta_i \geq 0, \quad \beta_{ij} \geq 0, \quad i, j = a, f, \quad i \neq j.$$

We observe that the functions P_a and P_f saturate, and to ensure that the functions P_i are positive for all market volumes (Y, H) we impose the requirements

$$\lim_{Y,H\to+\infty} P_a(Y, H) = A_a - \beta_a B_a - \beta_{af} D_a \equiv G_a > 0,$$

$$\lim_{Y,H\to+\infty} P_f(H, Y) = A_f - \beta_f B_f - \beta_{fa} D_f \equiv G_f > 0, \tag{11}$$

We notice that P_a and P_f are decreasing and convex function of the fishery market volume Y and farmed market volume H. Moreover, the positive constant A_i, $(i = a, f)$ is interpreted as consumers maximum willingness to pay. β_i and β_{ij} are non-negative parameters with the following interpretation: The coefficients β_i, $(i = a, f)$ describe a standard down sloped demand mechanism, while the presence of finite β_{ij} where $i, j = a, f$ with $i \neq j$ suggests that there could be some negative cross-price impact between the wild fish and the farmed fish supply. The positive constants B_i, and D_i, $(i = a, f)$ determine the strength of the direct market volume impact and the cross-volume market impact respectively. This means that as the quantity of farmed (harvested) fish increases, the lower is the marginal willingness to pay for the wild (farmed) fish when $\beta_{fa} > 0$ ($\beta_{af} > 0$). The positive constants G_i $(i = a, f)$ are interpreted as the saturation levels (minimum levels) of product marked price for the aquaculture and fishery products, respectively. The special case with $\beta_i = \beta_{ij} = 0$ $(i = a, f)$ is the case with constant product prices, i.e., the situation with perfect elastic demand in both product markets. The special case with $\beta_i > 0$, $\beta_{ij} = 0$ $(i = a, f)$ is the case with separate price formation, i.e., the marginal willingness to pay is only dependent of the market volume for each of the markets isolated which means no cross-market interdependence between the market for aquaculture products and fishery products.

We assume market equilibrium in both industries, i.e., that the supply is equal to the demand, for all time t. Furthermore, we assume an exogenous given price per unit of effort for each sector, w_i $(i = a, f)$, and define the profit π_a in the aquaculture industry and the profit in the fish harvest industry π_f by

$$\pi_a = P_a Y - w_a E_a, \quad \pi_f = P_f H - w_f E_f. \tag{12}$$

We must impose the profit condition in fisheries

$$qKG_f > w_f \tag{13}$$

which expresses the fact that the income per unit effort in harvesting has to exceed the cost per unit effort in the fishery. The left hand side of the inequality expresses the income per unit effort, when the fish stock is equal to the carrying capacity and market price realized at the saturation level, G_f.

In addition, we notice that the condition (13) implies the inequality

$$qK(A_f - \beta_{fa} D_f) > w_f. \tag{14}$$

The inequalities in (13)–(14) are referred to as the *profitability conditions*.

2.3. The open access regime

The open access regime consists of prescribing simplified dynamics for the effort variables E_f and E_a. We do this by assuming free entry and exit in proportion to profit for the fishery. Each of the fishing firms is supposed to consider the product price as given in the market. The expansions and the contractions of effort in the fishery sector correlate with positive and negative profits, and these adjustments include frictions and delays. We take these properties into account by suggesting the instantaneous change of rate of E_f to be proportional with the time-dependent sector profit π_f, i.e.,

$$\frac{dE_f}{dt} = \lambda_f [P_f qXE_f - w_f E_f]. \tag{15}$$

Here λ_f is the 'speed of adjustment' in the fishery[3]. By inserting the P_f - function defined by (9) and the production functions given as (1) and

[3] Smith (1969) states that the entry-speed coefficient is not necessarily equal to the exit-speed parameter. In order to simplify the problem we will consider a common entry-exit parameter λ_f. Similar types of enter-exit mechanisms concerning effort are often used in fishery studies, e.g. Chakraborty et al. (2012), Ghosh and Kar (2014) and Regnier and Schubert (2016).

(5) into (15) we obtain

$$\frac{dE_f}{dt} = E_f \lambda_f \left[\left(G_f + \beta_f B_f^2 \frac{1}{qXE_f + B_f} + \beta_{fa} D_f^2 \frac{1}{rE_a^{\frac{1}{2}} + D_f} \right) qX - w_f \right] \tag{16}$$

as the dynamical evolution equation for the effort variable E_f.

The goal of the firms in the aquaculture industry is to choose the effort E_a which maximizes the profit π_a. In line with the standard assumption in perfect competitive models, the industries are supposed to consist of many small firms where each of them is producing so small quantities that their behavior (regarding each of the actual chosen quantities) does not affect the market prices. This means that each firm is a price taker. However, higher and lower quantities in the total markets, consisting of all supplying firms, do affect the total supply, and hence the market equilibrium prices. From (1) and (12) we find that the profit maximizing condition reads

$$\frac{\partial \pi_a}{\partial E_a} = \frac{1}{2} P_a r E_a^{-\frac{1}{2}} - w_a = 0. \tag{17}$$

We now prescribe the dynamical evolution of the effort E_a in such a way that the instantaneous change of rate of E_a is proportional to $\frac{\partial \pi_a}{\partial E_a}$ i.e.

$$\frac{dE_a}{dt} = \lambda_a \frac{\partial \pi_a}{\partial E_a} = \lambda_a \left[\frac{1}{2} P_a r E_a^{-\frac{1}{2}} - w_a \right].$$

Here the positive proportionality constant λ_a determined by the 'speed of adjustment' measures the intensity of reaction for the aquaculture industry. This means that we tacitly assume that the equilibrium state of our modeling framework represents a scenario with profit maximization. By inserting the expression for P_a - function defined by (9) and the production functions given as (1) and (5) into (17) we end up with the rate equation

$$\frac{dE_a}{dt} = \lambda_a \left[\left(G_a + \beta_a B_a^2 \frac{1}{rE_a^{\frac{1}{2}} + B_a} + \beta_{af} D_a^2 \frac{1}{qXE_f + D_a} \right) \frac{1}{2} r E_a^{-\frac{1}{2}} - w_a \right] \tag{18}$$

for the effort variable E_a. Notice that the parameters (λ_a and λ_f) may be different, since the 'speed of adjustment' for each industry depends on conditions which may vary, including regulatory policy in both sectors.

Our model is summarized in the 4*D* nonlinear autonomous dynamical system (7), (8), (16) and (18). The variables and the parameters in the model are listed in Table 1. The measurement units given in Table 1 are *T* for time (e.g. *year, month*), *M* (e.g. *ton, kg*), *E* for effort (e.g. *employee, capital*) and currency *C* (e.g. *Euro, Yuan* etc.)

3. Analysis of the model

3.1. Scaling and general properties of the model

We scale the model (7), (8), (16) and (18) by following the procedure outlined, in Logan (1987). We proceed as follows: Introduce the dimensionless quantities τ, ξ, η, θ and ψ defined by

$$\tau = \sigma t, \quad X(t) = K\xi(\tau), \quad E_f = \frac{\sigma}{q}\theta(\tau),$$
$$E_a(t) = \left[\frac{K\sigma}{r}\right]^2 \left[\eta(\tau)\right]^2, \quad S(t) = K\psi(\tau), \tag{19}$$

and the dimensionless, positive parameters γ_n, $n = 1, 2, \ldots, 14$ defined and interpreted in Table 2.

We then end up with the 4*D* autonomous dynamical system

$$\frac{d\xi}{d\tau} = \xi \mathcal{F}(\xi, \theta, \eta, \psi), \tag{20}$$

Table 1
The aquaculture-fishery model. The fundamental units are *T* for time (e.g. *year, month*), *M* for mass (e.g. *tons, kg*), *E* for effort (e.g. *employee, capital*) and *C* for currency (e.g. *Euro, Yuan* etc.)

Variables/ parameters	Biological/ economical interpretation	Measurement units (dimensions)
t	Time	T
Y	Total aquaculture production volume	MT^{-1}
S	The harmful substance density (stock of pollutant)	M
Z	The flow of pollution from aquaculture production	MT^{-1}
X	Fish population density	M
K	Carrying capacity of the fish biomass	M
H	Production volume(harvest) in fishery	MT^{-1}
E_f	Effort(capital and labour) input in fishery	E
E_a	Effort(capital and labour) input in aquaculture	E
P_i	Market value of product i ($i = a, f$)	CM^{-1}
σ	Intrinsic growth rate for the biomass	T^{-1}
α	Growth-retardation parameter	1
q	Harvest efficiency rate	$E^{-1}T^{-1}$
r	Aquaculture efficiency rate	$ME^{-1/2}T^{-1}$
ϱ	Emission (pollution) parameter	1
ρ	Remediation (natural absorptive ability) rate	M^2T^{-1}
$g(S; d)$	Remediation capacity	M^{-1}
d	Remediation capacity parameter	M
β_i	Direct market price-volume impact in sector i ($i = a, f$)	$CM^{-2}T$
$\beta_{i,j}$	Cross market price-volume impacts $(i, j = a, f), (i \neq j)$	$CM^{-2}T$
A_i	Maximum willingness to pay, product i ($i = a, f$)	CM^{-1}
B_i	Direct price-saturation constant, product i ($i = a, f$)	MT^{-1}
D_i	Cross price-saturation constant, product i ($i = a, f$)	MT^{-1}
w_i	Exogenous cost per unit effort, sector i ($i = a, f$)	$CE^{-1}T^{-1}$
λ_f	Speed of adjustment, fishery	EC^{-1}
λ_a	Speed of adjustment, aquaculture industry	E^2C^{-1}

Table 2
Definition and interpretation of the nondimensional parameters γ_n, $n = 1, 2, \ldots, 14$ in the model (24)–(27).

Parameter definition	Interpretation
$\gamma_1 = \lambda_f q K G_f/\sigma$	Relative unit value of effort in fishery.
$\gamma_2 = \lambda_f q \beta_f B_f^2/\sigma^2$	Impact on fishery price from fishery volume.
$\gamma_3 = B_f/K\sigma$	Fishery price saturation parameter for the fishery volume.
$\gamma_4 = \lambda_f q \beta_{fa} D_f^2/\sigma^2$	Impact on fishery price from aquaculture volume.
$\gamma_5 = D_f/K\sigma$	Fishery price saturation parameter for the aquaculture volume.
$\gamma_6 = \lambda_f w_f/\sigma$	Relative unit cost of effort in fishery.
$\gamma_7 = \frac{\lambda_a G_a K}{4}\left[\frac{r}{\sigma K}\right]^4$	The relative unit value of effort in aquaculture
$\gamma_8 = \frac{\lambda_a \beta_a B_a^2}{4\sigma}\left[\frac{r}{\sigma K}\right]^4$	Impact on aquaculture price from aquaculture volume.
$\gamma_9 = B_a/K\sigma$	Aquaculture price saturation parameter for the aquaculture volume.
$\gamma_{10} = \frac{\lambda_a \beta_{af} D_a^2}{4\sigma}\left[\frac{r}{\sigma K}\right]^4$	Impact on aquaculture price from fishery volume.
$\gamma_{11} = D_a/K\sigma$	Aquaculture price saturation parameter for the fishery volume.
$\gamma_{12} = \frac{\lambda_a w_a}{2\sigma}\left[\frac{r}{\sigma K}\right]^2$	Relative unit cost of effort in aquaculture.
$\gamma_{13} = d/K$	Remediation capacity parameter.
$\gamma_{14} = \rho/K\sigma$	Relative emission rate.

$$\frac{d\theta}{d\tau} = \theta\mathcal{G}(\xi, \theta, \eta, \psi), \tag{21}$$

$$\frac{d\eta}{d\tau} = \mathcal{H}(\xi, \theta, \eta, \psi), \tag{22}$$

$$\frac{d\psi}{d\tau} = \mathcal{K}(\xi, \eta, \theta, \psi) \tag{23}$$

with the functions $\mathcal{F}$, $\mathcal{G}$, $\mathcal{H}$ and $\mathcal{K}$ given as

$$\mathcal{F}(\xi, \theta, \eta, \psi) = 1 - \xi - \theta - \alpha\psi, \tag{24}$$

$$\mathcal{G}(\xi, \theta, \eta, \psi) = \left[\gamma_1 + \frac{\gamma_2}{\xi\theta + \gamma_3} + \frac{\gamma_4}{\eta + \gamma_5}\right]\xi - \gamma_6, \tag{25}$$

$$\mathcal{H}(\xi, \theta, \eta, \psi) = \left[\gamma_7 + \frac{\gamma_8}{\eta + \gamma_9} + \frac{\gamma_{10}}{\xi\theta + \gamma_{11}}\right]\eta^{-2} - \gamma_{12}\eta^{-1}, \tag{26}$$

$$\mathcal{K}(\xi, \theta, \eta, \psi) = \varrho\eta - \gamma_{14}R(\psi; \gamma_{13}) \tag{27}$$

where

$$R(\psi; \gamma_{13}) = \frac{\psi}{\psi^2 + \gamma_{13}^2}. \tag{28}$$

The function R is referred to as the *nondimensional remediation capacity*. Notice the relationship between this function and the remediation capacity:

$$g(K\psi; K) = K^{-1}g(\psi; \gamma_{13}, 1) = K^{-1}R(\psi; \gamma_{13}). \tag{29}$$

Notice that the condition (13) translates into the constraint

$$\gamma_1 > \gamma_6 \tag{30}$$

on the dimensionless parameters γ_1 and γ_6. The profitability condition from the fishery (14) expressed in terms of the dimensionless quantities is given as

$$\frac{\gamma_1}{\gamma_6} + \frac{\gamma_2}{\gamma_3\gamma_6} = \frac{qK}{w_f}(G_f + \beta_f B_f) = \frac{qK}{w_f}(A_f - \beta_{fa}D_f) > 1 \tag{31}$$

Moreover, we classify the dimensionless parameters into the following four groups according to their roles in the model:

- **Group 1:** Parameter capturing the possible pollution biomass impact (*growth-retardation parameter*): α.
- **Group 2:** Parameters in the fishery sector of the model: $\gamma_1, \ldots, \gamma_6$.
- **Group 3:** Parameters in the aquaculture sector of the model: $\gamma_7, \ldots, \gamma_{12}$.
- **Group 4:** Parameters capturing the aquaculture production and the related pollution and remediation: ϱ, γ_{13}, γ_{14}.

In accordance with this classification a schematic visualisation of the interaction between the different components in the model (20)–(29) is displayed in Fig. 1. We notice that the Group 1 parameter i.e. the growth-retardation parameter α plays a key role in the model. It captures the ecological interdependence between aquaculture and fishery. Absence of this interaction ($\alpha = 0$), means that only the market interdependence is present.

Moreover, since the component functions $\mathcal{F}, \mathcal{G}, \mathcal{H}$ and $\mathcal{F}$ defined by (24)–(27) are smooth functions on the set

$$\Sigma = \{(\xi, \theta, \eta, \psi) \in \mathbb{R}^4; \eta \neq 0\}.$$

the initial value problem of the system (20)–(23) is, in accordance with Picards theorem, locally wellposed in Σ. In Appendix A we prove that any orbit of this system starting in the subset Σ_{inv} of the phase space defined by

$$\Sigma_{inv} = \{(\xi, \theta, \eta, \psi) \in \mathbb{R}^4; \xi \geq 0, \theta \geq 0, \eta > 0, \psi \geq 0\}$$

remains in that subset.

In the subsequent sections we will investigate the existence and linear stability of equilibrium states of the present model. The stability issue is resolved in the standard way by means of the spectral properties of the Jacobian $\mathbb{J}_4$ of the vector field $\mathbf{F}$ where

$$\mathbf{F}(\mathbf{x}) = (\xi\mathcal{F}(\mathbf{x}), \theta\mathcal{G}(\mathbf{x}), \mathcal{H}(\mathbf{x}), \mathcal{K}(\mathbf{x}))^T. \tag{32}$$

Here $\mathbf{x}$, $=(\xi, \theta, \eta, \psi)$. We will also present some numerical examples in the subsequent sections. The purpose of these illustrations is to facilitate interpretations of general results and visualize the model mechanisms.

The fundamental parameters belonging to the fishery part of the model are chosen such that the commercial fishery might be profitable. These parameters are listed in Table 3. By inserting these values into (19), we find that $\gamma_1 = 2$, $\gamma_6 = 1$ and consequently $\gamma_1/\gamma_6 = 2$, which is in agreement with the condition (13). For the remaining parameters listed in Table 1, it seems not possible to find estimates based on observations or experiments.

In Table 4 we have listed the input parameters $\gamma_1, \ldots, \gamma_{14}$ which will be used in the subsequent sections, together with ϱ, i.e., the Group 2 - Group 4 parameters. The Group 2 pair (γ_1, γ_2) and the Group 3 pair (γ_7, γ_{12}) measure the initial profitability in the fishery industry and the aquaculture industry, respectively. The values in both industries are chosen in agreement with the profitability conditions in (13). Furthermore, the Group 2 pair (γ_2, γ_4) and the Group 3 pair (γ_8, γ_{10}) describe how the market volume influences the market prices. γ_2 and γ_8 capture the direct volume effect in the fishing industry and the aquaculture industry, respectively. The parameters γ_4 and γ_{10} describe the cross-industry volume effect in the fishing industry and the aquaculture industry, respectively. According to market theory, it is reasonable to assume that the direct volume impact is more significant than the cross industry impact, see for instance Gravelle and Rees (2004). The values listed in Table 4 are selected in accordance with this assumption. The growth-retardation parameter α is varied throughout the whole manuscript, thus reflecting that our goal is to study the properties of the fundamental model as function of the growth-retardation mechanism.

3.2. Special cases

To elaborate on the mechanisms present in our model, it is useful to consider simplified versions of the model. In line with that we will first focus on the model in the case with only aquaculture production present i.e. when $\xi = \theta \equiv 0$ (Section 3.2.1) and the case with no effort in the fishery i.e. when $\theta \equiv 0$ (Section 3.2.2). In particular, we will investigate the existence and stability of equilibrium points within the frameworks of these simplified models and pinpoint at the role of these results within the full model. It turns out that we in the forthcoming analysis of this equilibrium problem will extensively make use of the condition $\mathcal{K}(\xi, \theta, \eta, \psi) = 0$ expressed on the form

$$R(\psi; \gamma_{13}) \equiv \frac{\psi}{\psi^2 + \gamma_{13}^2} = \frac{\varrho\eta}{\gamma_{14}} \tag{33}$$

Here we have made use of (27) and (28). We readily obtain

$$\psi = \psi_{\pm} \equiv \frac{1}{2\varrho\eta}\left[\gamma_{14} \pm \sqrt{\gamma_{14}^2 - 4\varrho^2\gamma_{13}^2\eta^2}\right] \tag{34}$$

from (33). Table 5 shows the number of positive solutions of this equation as a function of the positive input parameter $\frac{\varrho\eta}{\gamma_{14}}$.

We also notice that the nondimensional remediation capacity R attains its maximal value $R_{\max} = (2\gamma_{13})^{-1}$ for $\psi = \gamma_{13}$. This means that $\psi_- < \gamma_{13}$ (corresponding to $R'(\psi_-, \gamma_{13}) > 0$), whereas $\psi_+ > \gamma_{13}$ (corresponding to $R'(\psi_-, \gamma_{13}) < 0$). Here we tacitly assume that $\psi_{\pm}$ is given by (34) in the regime $0 < \eta < \frac{\gamma_{14}}{2\varrho\gamma_{13}}$.

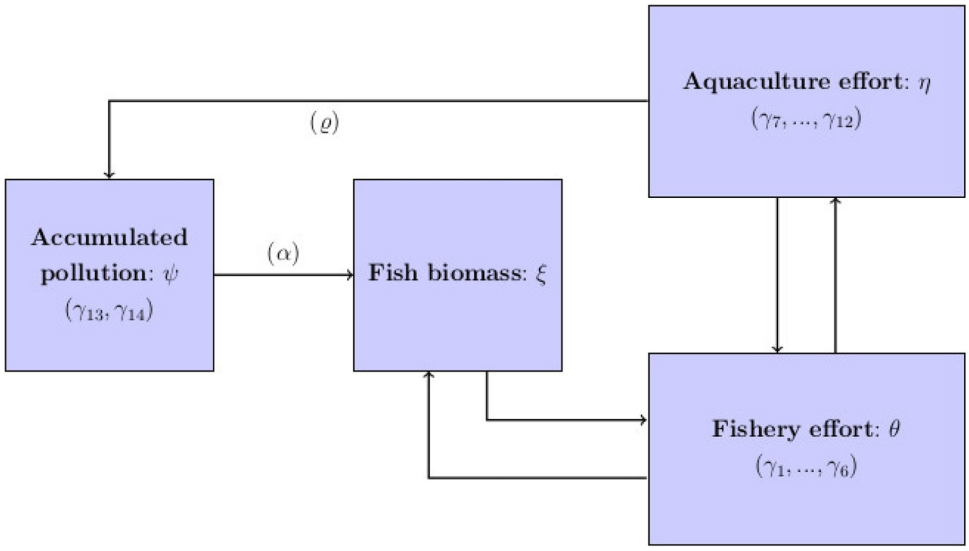

Fig. 1. The interaction scheme for the model (20)–(29).

Table 3
Example values of fundamental parameters for the fishery part of the model. The measurement units are $M = Ton$, $C = Euro$, $E = Vessels$ and $T = Year$.

Parameters	Values	Units
K	40000000	M
G_f	1000	CM^{-1}
q	0.000002	$E^{-1}T^{-1}$
λ_f/σ	0.000025	ETC^{-1}
w_f	40000	$CE^{-1}T^{-1}$

3.2.1. The case with only aquaculture production ($\xi = \theta \equiv 0$)

We first consider the case with isolated activity in the fish farming industry. This means that we neglect the effects of the biomass and the effort in the fishery, i.e., we assume that $\xi = \theta \equiv 0$. In this case the dynamical evolution is governed by the 2D subsystem

$$\frac{d\eta}{d\tau} = f_2(\eta; \hat{\eta}_\pm), \tag{35}$$

$$\frac{d\psi}{d\tau} = \varrho\eta - \gamma_{14}R(\psi; \gamma_{13}) \tag{36}$$

where the function f_2 is defined as

$$f_2(\eta; \hat{\eta}_\pm) \equiv -\frac{\gamma_{12}}{\eta^2(\eta + \gamma_9)}(\eta - \hat{\eta}_-)(\eta - \hat{\eta}_+). \tag{37}$$

Here

$$\hat{\eta}_\pm = \frac{\gamma_{10}}{2\gamma_{11}\gamma_{12}} + \frac{1}{2\gamma_{12}}\left[\gamma_7 - \gamma_9\gamma_{12} \pm \sqrt{\frac{\gamma_{10}^2 + 2\gamma_{10}\gamma_{11}(\gamma_7 + \gamma_9\gamma_{12})}{\gamma_{11}^2} + D}\right] \tag{38}$$

with D given by

$$D = (\gamma_7 + \gamma_9\gamma_{12})^2 + 4\gamma_8\gamma_{12}. \tag{39}$$

We notice that $\hat{\eta}_- < 0 < \hat{\eta}_+$. For the Group 3 parameters listed in Table 4, we find that $\hat{\eta}_- = -0.6712$ and $\hat{\eta}_+ = 2.4212$. According to Table 5, we get equilibrium points in the first quadrant of the ψ, η-plane of the subsystem (35)–(36) if

$$\hat{\eta}_+ \le \frac{\gamma_{14}}{2\varrho\gamma_{13}}. \tag{40}$$

These equilibrium points are given by (ψ_1, η_1) where $\eta_1 = \hat{\eta}_+$ and $\psi_1 = \psi_\pm$ with $\eta = \eta_1$. For the Group 3 and Group 4 parameters listed in Table 4 we notice that the condition (40) is fulfilled.

For the 2D system (35)–(36), we recover the result of Bergland et al. (2019): In accordance with Table 5 the actual subsystem possesses up to two equilibrium states located in the first quadrant in the ψ, η -plane. Let us assume that we are in the regime with at least one equilibrium point. We first observe that we always have $f_2'(\eta_1; \hat{\eta}_\pm) < 0$[4]. Thus stability of the equilibrium state of the 2D system relies on the monotonicity property of the remediation function evaluated at the solution of (33): For $R'(\psi_1; \gamma_{13}) > 0$, the equilibrium point is asymptotically stable, whereas for the negative slope condition $R'(\psi_1; \gamma_{13}) < 0$ we have instability of the corresponding equilibrium point.

The two equilibrium points are depicted on the phase portrait (Fig. Fig. 2) marked A (asymptotically stable) and B (unstable) respectively. Numerical run (Fig. 3) illustrates stabilization of the equilibrium point A.

Let us then study the role of the aquaculture-pollution system (35)–(36) as a part of the full system (20)–(29). We first notice that the points $Q_1^{(\pm)}$ defined by

$$Q_1^{(\pm)} = (0, 0, \hat{\eta}_+, \psi_\pm) \tag{41}$$

is a boundary equilibrium point of the system (20)–(29). The Jacobian of the vectorfield **F** defined by (32) evaluated at $Q_1^{(\pm)}$ assumes the lower triangular form

$$\mathbb{J}_4(Q_1^{(\pm)}) = \begin{pmatrix} \psi_\pm(\alpha_\pm^{(1)} - \alpha) & 0 & 0 & 0 \\ 0 & -\gamma_6 & 0 & 0 \\ 0 & 0 & f_2'(\hat{\eta}_+; \hat{\eta}_\pm) & 0 \\ 0 & 0 & \varrho & -\gamma_{14}R'(\psi_\pm; \gamma_{13}) \end{pmatrix}. \tag{42}$$

Here

$$\alpha_\pm^{(1)} \equiv \frac{1}{\psi_\pm} \tag{43}$$

where we notice that $\alpha_+^{(1)} < \alpha_-^{(1)}$. We have also made use of the estimate for the partial derivative $\frac{\partial\mathcal{H}}{\partial\eta}$ evaluated at the equilibrium point $Q_1^{(\pm)}$:

$$\frac{\partial\mathcal{H}}{\partial\eta}(Q_1^{(\pm)}) = -\left[\frac{\gamma_8}{\eta_1 + \gamma_9} + \gamma_{12}\right]\hat{\eta}_+^{-2} = f_2'(\hat{\eta}_+; \hat{\eta}_\pm) < 0.$$

This is consistent with the fact that $f_2'(\hat{\eta}_+; \hat{\eta}_\pm) < 0$.

We conclude that $Q_1^{(+)}$ will be unstable for all $\alpha \neq \alpha_+^{(1)}$ since the

[4] Here and in the sequel we will make use of the notation $f_2' \equiv \frac{df_2}{d\eta}$ and $R' \equiv \frac{dR}{d\psi}$.

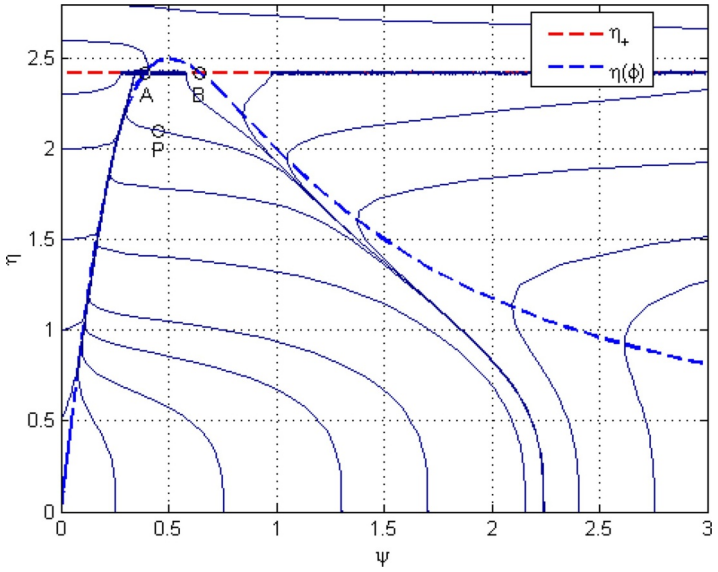

Fig. 2. The phase portrait of the subsystem (35)–(36). Input parameters are given as Group 3-Group 4 in Table 4. The nullcline $\eta = \hat{\eta}_+$ and the nullcline $\eta = \frac{\gamma_{14}}{\varrho} R(\psi; \gamma_{13})$ together with the equilibrium points $A = (2.4212, 0.3877)$ and $B = (2.4212, 0.6449)$ of the subsystem (35)–(36) are displayed. The point $P = (2.1, 0.45)$ is the initial condition for the numerical simulations underlying Fig. 3.

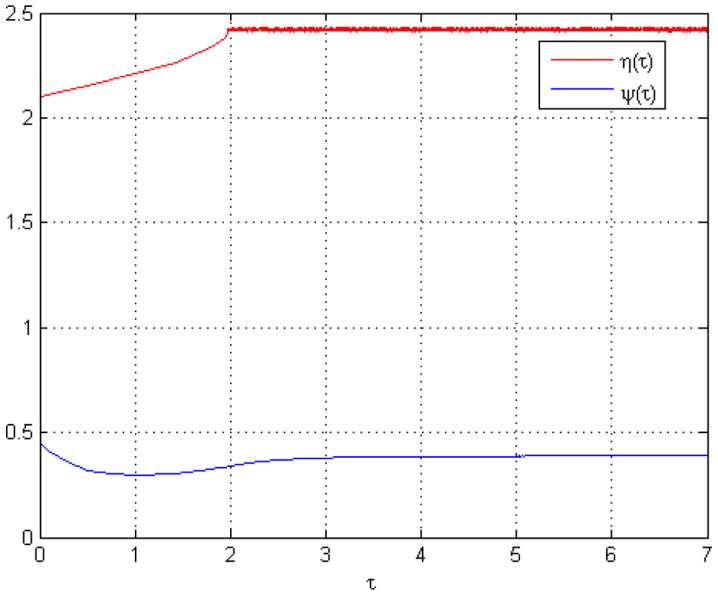

Fig. 3. Numerical example illustrating the behavior of the subsystem (35)–(36). The nondimensional production variable η (red curve) and nondimensional accumulated pollution ψ (blue curve) as function of the nondimensional time τ. Initial condition $P = (\eta, \psi) = (2.1, 0.45)$ is marked in Fig. 2.

negative slope condition $R'(\psi_+; \gamma_{13}) < 0$ is always fulfilled in this case. As a consequence of Shoshitaishvilis theorem,[5] this conclusion also holds true in the case $\alpha = \alpha_+^{(1)}$, when the corresponding equilibrium point Q_1^+ is a non-hyperbolic equilibrium point. The equilibrium point $Q_1^{(-)}$ is asymptotically stable within the framework of the system (20)–(29) if $\alpha > \alpha_-^{(1)}$. In the complementary parameter regime it will be unstable. In particular, one should notice that we will have instability of $Q_1^{(-)}$ if $\alpha_-^{(1)} > \alpha$ i.e. even in the regime where the positive slope condition $R'(\psi_-; \gamma_{13}) > 0$ is fulfilled. The transition case $\alpha = \alpha_-^{(1)}$ represents a static codimension 1-bifurcation point. We observe that $rank\{\mathbb{B}_1\} = 3$ for $\alpha = \alpha_-^{(1)}$ where $\mathbb{B}_1$ is the Jacobian $\mathbb{J}_4(Q_1^{(-)})$ evaluated at the bifurcation point, extended with the column vector $\frac{\partial \mathbf{F}}{\partial \alpha}(\alpha = \alpha_-^{(1)})$ where $\mathbf{F}$ is the vector field defined by (32), i.e.,

$$\mathbb{B}_1 = \begin{pmatrix} 0 & 0 & 0 & 0 & 0 \\ 0 & -\gamma_6 & 0 & 0 & 0 \\ 0 & 0 & f_2'(\hat{\eta}_+; \hat{\eta}_\pm) & 0 & 0 \\ 0 & 0 & \varrho & -\gamma_{14} R'(\psi_-; \gamma_{13}) & 0 \end{pmatrix}.$$

Since $\mathbb{B}_1$ has not a maximal rank, we will get a static codimension - 1 bifurcation which is not a saddle node bifurcation for $\alpha = \alpha_-^{(1)}$. In the next subsubsection it will be clear that the actual bifurcation in accordance with Logan (1987) turns out to be a transcritical bifurcation.

Notice that the stability results for (41) are sensible from the perspective of economics: The condition $\alpha > \alpha_-^{(1)}$ means a high pollution effect from the aquaculture compared to the remediation capacity. In this state the potential growth in the fish stock is harmed by the pollution from aquaculture. Hence, the fish stock is negligible, and consequently there should be no effort in the fishery activity.

This interpretation is supported by the numerical results for the full

[5] See Chapter 6 in Arnold (1988).

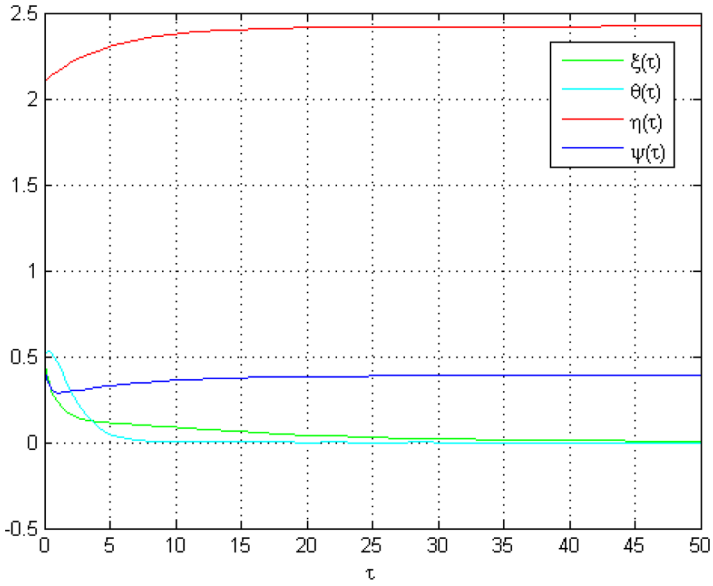

Fig. 4. Numerical example illustrating the behavior of the full system the system (20)–(29). The nondimensional biomass variable ξ (green), the nondimensional effort variable θ (turquoise), the nondimensional effort variable η (red) and the nondimensional accumulated pollution ψ (blue curve) as function of the nondimensional time τ. Input parameters are given as Group 2 - Group 4 in Table 4 and $\alpha = 2.7$. The initial condition is $(\xi, \theta, \eta, \psi) = (0.5, 0.5, 2.1, 0.45)$. Notice that the η - and ψ - coordinate of the initial condition are the same as for the simulations underlying Fig. 3.

system: For the input parameters in Group 2 - Group 4 in Table 4 the equilibrium points of the type Q_1 are given as

$$Q_1^{(+)} = (0, 0, 2.4212, 0.6449), \quad Q_1^{(-)} = (0, 0, 2.4212, 0.3877).$$

Moreover, simple computation shows that $\alpha_-^{(1)} = 2.5796$ in this case. $Q_1^{(+)}$ is unstable whereas $Q_1^{(-)}$ is stable (unstable) if $\alpha > 2.5796$ ($0 \leq \alpha < 2.5796$).

We then run the full model (20)–(29) with initial condition in the vicinity of the two equilibrium points $Q_1^{(+)}$ and $Q_1^{(-)}$ with $\alpha > \alpha_-^{(1)}$. The outcome of these computations is summarized in Fig. 4. We clearly see that the temporal evolution settles down on a state which is identified as $Q_1^{(-)}$, thus confirming the predictions obtained from the theoretical analysis. Fig. 4 illustrates the outcome of a situation with strong growth-retardation influences. Here the initial biomass and fishery effort are not sustainable. The accumulated pollution level inhibits stock growth and thereby makes the fishery unprofitable. The temporal evolution of the biomass and effort settles down on the stable equilibrium $Q_1^{(-)}$. This development involves a relatively rapid decrease in the nondimensional effort (θ) and nondimensional biomass (ξ). Both the fishery effort and the fish stock are wiped out within finite time.

3.2.2. The case with no effort in the fishery ($\theta \equiv 0$)

Let us consider the case with finite biomass present but with no harvest activity in the fishing industry. This means that $\theta \equiv 0$. The dynamical system (20)–(29) restricted to the hyperplane $\theta = 0$ simplifies to the 3*D* system

$$\frac{d\xi}{d\tau} = \xi(1 - \xi - \alpha\psi), \tag{44}$$

$$\frac{d\eta}{d\tau} = f_2(\eta; \hat{\eta}_\pm), \tag{45}$$

$$\frac{d\psi}{d\tau} = \varsigma\eta - \gamma_{14}R(\psi; \gamma_{13}) \tag{46}$$

in this case.

Here f_2 is defined by (37). We observe that this system possesses equilibrium points of the type $(1 - \alpha\psi_2, \eta_2, \psi_2)$ where $\eta_2 = \hat{\eta}_+$ is given by means of (38)–(39), whereas $\psi_2 = \psi_\pm$ is given by (34) with $\eta = \eta_2$. We notice that $\eta_2 = \eta_1$ and $\psi_2 = \psi_1$ where ψ_1 and η_1 are defined in Section 3.2.1. Here we tacitly assume that we are in the parameter regime for which the roots (34) are real. Moreover, we assume that $0 \leq \alpha < \alpha_\pm^{(1)}$ in order to ensure that the coordinates of the actual equilibrium point are positive.

In order to assess the stability of the equilibrium points of the system (44)–(46), we proceed in the standard way by computing the Jacobian matrix of the vector field defining this system. Doing this we obtain

$$\mathbb{J}_3 = \begin{pmatrix} -\psi_\pm(\alpha_\pm^{(1)} - \alpha) & 0 & -\alpha\psi_\pm(\alpha_\pm^{(1)} - \alpha) \\ 0 & f_2'(\eta_+; \hat{\eta}_\pm) & 0 \\ 0 & \varsigma & -\gamma_{14}R'(\psi_\pm; \gamma_{13}) \end{pmatrix} \tag{47}$$

from which it follows that only the equilibrium point $(1 - \alpha\psi_-, \hat{\eta}_+, \psi_-)$ is asymptotically stable within the framework of (44)–(46).

We then notice that the subsystem (45)–(46) is identical with the system (35)–(36). This means that the dynamical evolution as prescribed by means of (44)–(46) can be studied by viewing (45)–(46) as an input to the modified logistic Eq. (44). The solution of the equation (44) with $\xi(0) = \xi_0$ can easily be found by elementary techniques. We readily find that

$$\xi(\tau, \alpha) = \frac{\xi_0 \exp[f(\tau, \alpha)]}{\xi_0 \int_0^\tau \exp[f(s, \alpha)]ds + 1} \tag{48}$$

where

$$f(\tau, \alpha) \equiv \tau - \alpha \int_0^\tau \psi(s)ds. \tag{49}$$

We then investigate the level curves for the biomass function $\xi = \xi(\tau, \alpha)$ given by (48)–(49) on the interval $[0, \alpha_-^{(1)})$. The outcome of this study is summarized in the plot depicted in Fig. 5. Here we have used the Group 3 - Group 4 in Table 4 and the initial condition $P = (2.1, 0.45)$ for the purpose of constructing the input function ψ in the modified logistic Eq. (44). Notice that this means that graph of the input function ψ is the same as the graph displayed in Fig. 3. The result depicted in Fig. 5 demonstrates the role of the growth-weakening mechanism in the model. In the case of no fishery effort (and no harvest volume), an increase in the growth-retardation parameter α, means a decrease in the biomass density as a function of time.

Finally we consider the stability of the equilibrium points $Q_2^{(\pm)}$ defined as

$$Q_2^{(\pm)} = (\psi_\pm(\alpha_\pm - \alpha), 0, \hat{\eta}_+, \psi_\pm) \tag{50}$$

within the framework of the full system (20)–(29). The Jacobian for

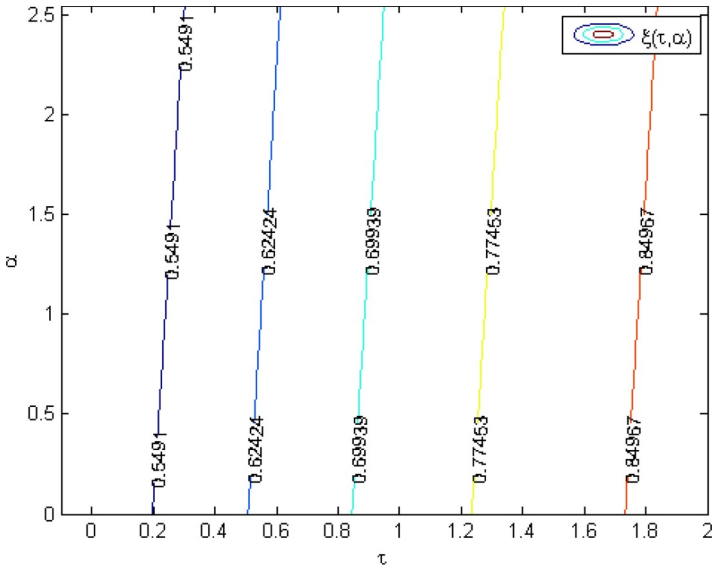

Fig. 5. The level curves for the nondimensional biomass $\xi(\tau, \alpha) = \hat{\xi}$ on the interval $[0, \alpha_{-}^{(1)})$. The function $\xi(\tau, \alpha)$ is given by (48)–(49). The labels attached to the level curves are the level curve constants $\hat{\xi}$. For the purpose of constructing the input function ψ in the modified logistic Eq. (44), the input parameters are Group 3 - Group 4 in Table 4 and the initial condition $P = (2.1, 0.45)$ for the subsystem (35)–(36).

these equilibrium points reads

$$\mathbb{J}_4(Q_2^{(\pm)}) = \begin{pmatrix} -\psi_{\pm}(\alpha_{\pm}^{(1)} - \alpha) & -\psi_{\pm}(\alpha_{\pm}^{(1)} - \alpha) & 0 & -\alpha\psi_{\pm}(\alpha_{\pm}^{(1)} - \alpha) \\ 0 & \mathcal{G}(Q_2^{\pm}) & 0 & 0 \\ 0 & -\frac{\gamma_8\psi_{\pm}(\alpha_{\pm}^{(1)} - \alpha)}{\gamma_{11}^2\hat{\eta}_{+}^2} & f_2'(\eta_{+}; \hat{\eta}_{\pm}) & 0 \\ 0 & 0 & \varrho & -\gamma_{14}R'(\psi_{\pm}; \gamma_{13}) \end{pmatrix}. \tag{51}$$

Here $\mathcal{G}(Q_2^{(\pm)})$ is given as

$$\mathcal{G}(Q_2^{(\pm)}) = \psi_{\pm}(\alpha_{\pm}^{(1)} - \alpha)(\gamma_1 + \frac{\gamma_2}{\gamma_3} + \frac{\gamma_4}{\hat{\eta}_{+} + \gamma_5}) - \gamma_6.$$

The α-value for which $\mathcal{G}(Q_2^{(\pm)}) = 0$ is given by

$$\alpha = \alpha_{\pm}^{(2)} \equiv \alpha_{\pm}^{(1)}\left[1 - \frac{\gamma_6}{\gamma_1 + \frac{\gamma_2}{\gamma_3} + \frac{\gamma_4}{\hat{\eta}_{+} + \gamma_5}}\right]. \tag{52}$$

We notice that the profitability condition (31) implies that $\alpha_{+}^{(2)} < \alpha_{+}^{(1)}$ and $\alpha_{-}^{(2)} < \alpha_{-}^{(1)}$. Moreover, since $\alpha_{+}^{(1)} < \alpha_{-}^{(1)}$, we have $\alpha_{+}^{(2)} < \alpha_{-}^{(2)}$. For $\alpha = \alpha_{\pm}^{(2)}$, the corresponding equilibrium point $Q_2^{(\pm)}$ is a non-hyperbolic equilibrium point. In accordance with Hartman-Grobmans theorem[6] the negative slope condition $R'(\psi_{+}; \gamma_{13}) < 0$ implies that $Q_2^{(+)}$ is unstable for all $0 \leq \alpha < \alpha_{+}^{(1)}$ with $\alpha \neq \alpha_{+}^{(2)}$. Shoshitaishvilis theorem[7] implies that this also holds true in the non-hyperbolic case $\alpha = \alpha_{+}^{(2)}$. The stability property of $Q_2^{(-)}$ depends sensitively on the value of the growth-retardation parameter α. The equilibrium point $Q_2^{(-)}$ will be asymptotically stable provided $\alpha_{-}^{(2)} < \alpha < \alpha_{-}^{(1)}$. In the complementary regime it will be unstable. For $\alpha = \alpha_{-}^{(2)}$, we have $rank\{\mathbb{B}_2\} = 3$. where $\mathbb{B}_2$ is the Jacobian $\mathbb{J}_4(Q_2^{(-)})$ evaluated at the bifurcation point, extended with the column vector $\frac{\partial \mathbf{F}}{\partial \alpha}(\alpha = \alpha_{-}^{(2)})$ where $\mathbf{F}$ is the vector field defined by (32), i.e.,

$$\mathbb{B}_2 = \begin{pmatrix} -\xi_{-}^{(2)} & -\xi_{-}^{(2)} & 0 & -\alpha_{-}^{(2)}\xi_{-}^{(2)} & -\xi_{-}^{(2)}\psi_2 \\ 0 & 0 & 0 & 0 & 0 \\ 0 & -\frac{\gamma_8\xi_{-}^{(2)}\psi_2)}{\gamma_{11}^2\eta_2^2} & f_2'(\hat{\eta}_{+}; \hat{\eta}_{\pm}) & 0 & 0 \\ 0 & 0 & \varrho & -\gamma_{14}R'(\psi_{-}; \gamma_{13}) & 0 \end{pmatrix}.$$

where

$$\xi_{-}^{(2)} \equiv 1 - \alpha_{-}^{(2)}\psi_{-}.$$

This means that we have a static codimension - 1 bifurcation for $Q_2^{(-)}$ when $\alpha = \alpha_{-}^{(2)}$. As $\mathbb{B}_2$ has not maximal rank, we conclude that this bifurcation is not of the saddle-node type. The analysis carried out in Appendix C shows that $Q_2^{(-)}$ will be subject to a transcritical bifurcation for $\alpha = \alpha_{-}^{(2)}$.

For $\alpha = \alpha_{\pm}^{(1)}$, we notice that the equilibrium point $Q_2^{(\pm)}$ merges together with $Q_1^{(\pm)}$. For $\alpha = \alpha_{-}^{(1)}$, the stability analysis of $Q_1^{(-)}$ worked out in the previous subsubsection shows that the static codimension - 1 bifurcation detected for $\alpha = \alpha_{-}^{(1)}$ is a transcritical bifurcation. See e.g. Logan (1987) for more details.

For the input parameters in Group 2 - Group 4 in Table 4 and $\alpha_{-}^{(1)} = 2$ the boundary equilibrium point $Q_2^{(-)}$ for which the positive slope condition $R'(\psi_{-}, \gamma_{13}) > 0$ is fulfilled is given as

$$Q_2^{(-)} = (0.2246, 0, 2.4212, 0.3877).$$

Moreover, simple computation shows that $\alpha_{-}^{(2)} = 1.7402$ in this case. For the numerical runs leading to Fig. 6, we observe that $\alpha_{-}^{(2)} < \alpha < \alpha_{-}^{(1)}$. Moreover, we observe that the solution settles down on the equilibrium point $Q_2^{(-)}$ in a damped oscillatory manner. The findings summarized in Fig. 6 are thus consistent with the theoretical predictions deduced from the present stability analysis. The bioeconomic explanation is similar to the interpretation obtained from Fig. 4. The case in Fig. 6 describes a situation with weaker growth-retardation compared to Fig. 4. The initial coordinates of the biomass, the fishery effort and the accumulated pollution level are the same in both cases. In both cases the fishery effort becomes unprofitable in the long run. However, from the initial conditions, shown in Fig. 6, the fishery will be profitable causing a short run increased effort, which leads to a reduction in the biomass density. This together with the following market price fall makes the fishery unprofitable. The biomass and effort variables oscillate and relaxate towards the stable equilibrium $Q_2^{(-)}$, where the fishery effort is wiped

[6] See e.g. Guckenheimer and Holmes (1983) or Perko (2013).
[7] See Chapter 6 in Arnold (1988).

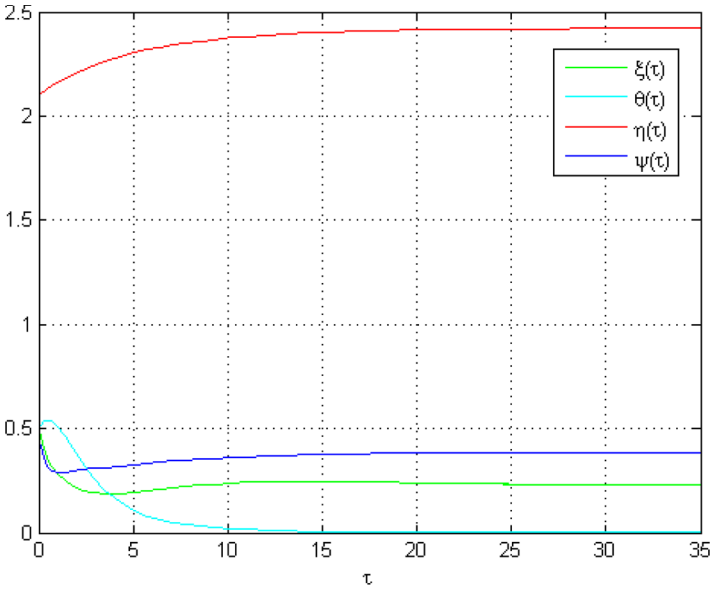

Fig. 6. Numerical example illustrating the behavior of the full system the system (20)–(29). The nondimensional biomass variable ξ (green), the nondimensional effort variable θ (turquoise), the nondimensional effort variable η (red) and the nondimensional accumulated pollution ψ (blue curve) as function of the nondimensional time τ. Input parameters are given as Group 2 - Group 4 in Table 4 and $\alpha = 2$. The initial condition is $(\xi, \theta, \eta, \psi) = (0.5, 0.5, 2.1, 0.45)$. Notice that the initial η - and ψ - coordinate are the same as for the simulations underlying Fig. 3.

out within finite time, whereas the biomass, in this state with no harvest activity and more moderate growth-retardation from pollution, survives and stabilizes on a finite value ($\xi = 0.2246$).

According to the discussion of possible stability of (50), the economic interpretation relates to the profitability of the fishery compared to the damage on the growth of the fish stock caused by the aquaculture production. From (52) we notice that $\alpha_{-}^{(2)}$ depends on parameters describing the profitability and the market responses in the fishery. More specifically, it means that a low potential marked value (represented by γ_1) or high costs (represented by γ_6) together with a considerable pollution effect from aquaculture on the fishery growth, could lead to a scenario where the fishery effort in the long run becomes unprofitable, and consequently it will be reduced to no activity.

3.2.3. Special cases regarding market interactions

Let us continue to elaborate on the market mechanisms present in the modelling framework by considering (i) the case with constant product prices, and ii) the case with separate price formation.

(i) The case with constant product prices.

The case with constant product prices is based on the assumption that the marginal willingness to pay is independent of the market volume, i.e., the situation with perfect elastic demand for both product markets. This parameter regime captures the situation when both the fishery and the aquaculture industry have a marginal impact on the total market for relevant products. By this assumption it follows that $\beta_i = 0$ and $\beta_{ij} = 0$, $(i, j = a, f)$ $(i \neq j)$. In the dimensionless setting these assumptions correspond to letting $\gamma_2 = \gamma_4 = \gamma_8 = \gamma_{10} = 0$.

In this case the dynamical system (20)–(29) simplifies to

$$\frac{d\xi}{d\tau} = \xi(1 - \xi - \theta - \alpha\psi), \tag{53}$$

$$\frac{d\theta}{d\tau} = \theta(\gamma_1\xi - \gamma_6), \tag{54}$$

$$\frac{d\eta}{d\tau} = \eta^{-2}\gamma_{12}\left(\frac{\gamma_7}{\gamma_{12}} - \eta\right), \tag{55}$$

$$\frac{d\psi}{d\tau} = \varrho\eta - \gamma_{14}R(\psi; \gamma_{13}). \tag{56}$$

For $\alpha = 0$, the 2*D* subsystem (53)–(54) becomes the standard Gordon - Schaefer model. That model has been extensively studied in many works. See e.g. Bergland et al. (2018, 2019) and the references therein.

The simplified model (53)–(56) possesses boundary equilibrium points of the type $Q_1^{(\pm)}$ and $Q_2^{(\pm)}$ with the same type of stability properties as detailed in the previous subsubsections. We readily find that

$$Q_1^{(\pm)} = \left(0,\ 0,\ \frac{\gamma_7}{\gamma_{12}},\ \psi_{\pm}\right),$$

$$Q_2^{(\pm)} = \left(\psi_{\pm}(\alpha_1^{(\pm)} - \alpha),\ 0,\ \frac{\gamma_7}{\gamma_{12}},\ \psi_{\pm}\right), \quad 0 \leq \alpha < \alpha_{\pm}^{(1)}.$$

Here

$$\psi_{\pm} = \frac{\gamma_{12}}{2\varrho\gamma_7}\left[\gamma_{14} \pm \sqrt{\gamma_{14}^2 - 4\varrho^2\gamma_{13}^2\gamma_7^2\gamma_{12}^{-2}}\right], \quad \alpha_{\pm}^{(1)} = 1/\psi_{\pm}. \tag{57}$$

In accordance with Table 5 we tacitly assume that we are in the parameter regime

$$\varrho \leq \frac{\gamma_{12}\gamma_{14}}{2\gamma_7\gamma_{13}},$$

so that we are guaranteed that $\psi_{\pm}$ are real. By proceeding in the same way as in the previous subsubsections we find that $Q_1^{(+)}$ and $Q_2^{(+)}$ are unstable. Moreover, $Q_1^{(-)}$ is asymptotically stable for $\alpha > \alpha_{-}^{(1)}$ and unstable for the complementary regime $0 \leq \alpha < \alpha_{-}^{(1)}$. Finally, but not least, $Q_2^{(-)}$ is asymptotically stable for $\alpha_{-}^{(2)} < \alpha < \alpha_{-}^{(1)}$ and unstable for $0 \leq \alpha < \alpha_{-}^{(2)}$. Here

$$\alpha_{\pm}^{(2)} = \alpha_{\pm}^{(1)}\left(1 - \frac{\gamma_6}{\gamma_1}\right). \tag{58}$$

Since $\frac{\gamma_6}{\gamma_1} < 1$, we observe that $\alpha_{-}^{(2)} < \alpha_{-}^{(1)}$. For the input parameters used in Table 4, we find that $\alpha_{-}^{(1)} = 4$ and $\alpha_{-}^{(2)} = 2$, which confirms this fact.

The system (53)–(56) possesses interior equilibrium points denoted by $Q_e^{(\pm)}$, i.e.,

$$Q_e = (\xi_e, \theta_e, \eta_e, \psi_e) \tag{59}$$

where

$$\xi_e = \frac{\gamma_6}{\gamma_1} < 1, \quad \theta_e = 1 - \xi_e - \alpha\psi_e, \quad \eta_e = \frac{\gamma_7}{\gamma_{12}} > 1,$$

$$\psi_e = \psi_{\pm} \equiv \frac{1}{2\varrho\eta_e}\left[\gamma_{14} \pm \sqrt{\gamma_{14}^2 - 4\varrho^2\gamma_{13}^2\eta_e^2}\right].$$

Here we tacitly assume that $\eta_e \leq \frac{\gamma_{14}}{2\varrho\gamma_{13}}$ so that $\psi_{\pm}$ is real and that $\alpha < \alpha_{\pm}^{(2)}$ in order to ensure that θ_e is positive. A simple analysis reveals that this equilibrium point with $\psi_e = \psi_{-}$ (corresponding to the positive

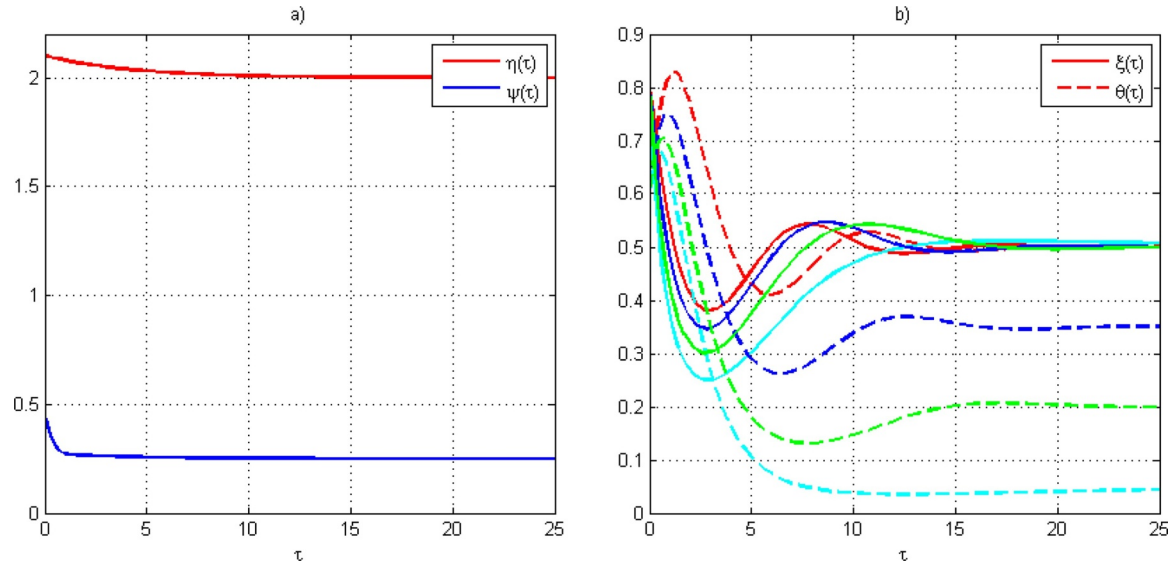

Fig. 7. Numerical example illustrating the behavior of the system (53)–(56) as a function of the growth-retardation parameter α. Input data in the computations are given in Table 4, except that we let $\gamma_2 = \gamma_4 = \gamma_8 = \gamma_{10} = 0$. The solution of subsystem (55)–(56) with initial condition $P = (\eta, \psi) = (2.1, 0.45)$ is depicted in Fig. 7a. Fig. 7b shows the temporal development of ξ and θ for $\alpha = 0$ (red), $\alpha = 0.6$ (blue), $\alpha = 1.2$ (green) and $\alpha = 1.8$ (turquoise) with ψ presented in Fig. 7a as an input function and $(\xi, \theta) = (0.8, 0.6)$ as initial condition.

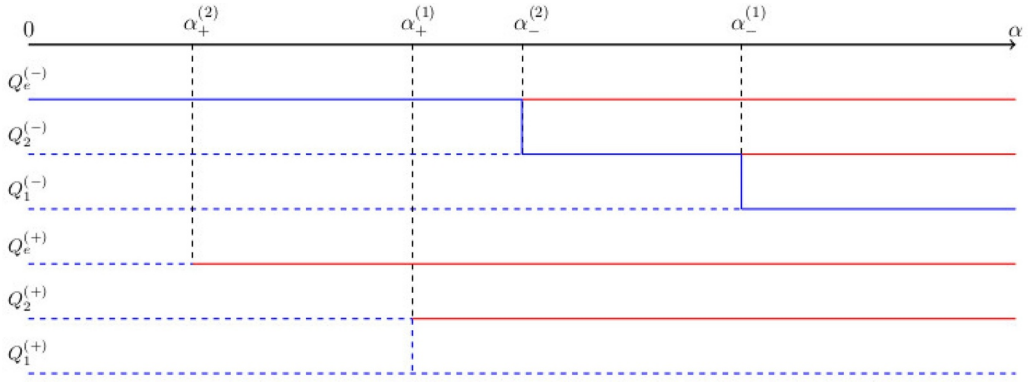

Fig. 8. Summary of the properties of the existence and stability of equilibrium states for the system (53)–(56), as function of the growth-retardation parameter α. Here $\alpha_1^{(\pm)}$ and $\alpha_1^{(\pm)}$ are given by (57) and (58), respectively. Horizontal blue line: Stable equilibrium states. Horizontal dotted line: Unstable equilibrium states. Horizontal red line: Non-existence of equilibrium states. Vertical blue lines at $\alpha = \alpha_2^{(-)}$ and $\alpha = \alpha_1^{(-)}$ correspond to $Q_e^{(-)}$ merging together with $Q_2^{(-)}$ and $Q_2^{(-)}$ merging together with $Q_1^{(-)}$, respectively, through transcritical bifurcation. Vertical dotted blue lines at $\alpha = \alpha_2^{(+)}$ and $\alpha = \alpha_1^{(+)}$ correspond to $Q_e^{(+)}$ merging together with $Q_2^{(+)}$ and $Q_2^{(+)}$ merging together with $Q_1^{(+)}$, respectively. Notice that the existence and stability theory for the equilibrium states in this case is qualitatively the same as in the general case (20)–(29).

slope condition $R'(\psi_-; \gamma_{13}) > 0$) is asymptotically stable, whereas it is unstable for $\psi_e = \psi_+$ (corresponding to the negative slope condition $R'(\psi_-; \gamma_{13}) < 0$).

Bearing the outcome of the equilibrium and stability analysis in mind, we study the initial value problem for the system (53)–(56) in the following way: We first solve the initial value problem of the 2D - subsystem (55)–(56). The initial condition for this system is close to the asymptotically stable equilibrium point (η_e, ψ_-) of this subsystem. The graphs of the solution to this system are displayed in Fig. 7a. We then solve the initial value problem of (53)–(54) with the ψ - component of the solution of (55)–(56) as an input function. In Fig. 7b the graphs of the solution to this system are depicted for different values of the growth-retardation parameter α. The input parameters used in the computations underlying these plots are given as in Table 4, except that we let $\gamma_2 = \gamma_4 = \gamma_8 = \gamma_{10} = 0$.

The case with constant prices in both product markets isolates the ecological interdependence between the aquaculture and the fishery. This is demonstrated in Fig. 7b. This means that we assume no market interaction between the industries and perfect elastic demand in both markets. A notable feature here is standard fishery adjustments under an open access regime and a constant fish price where the nondimensional biomass and effort variables oscillate. The biomass variable relaxates towards a level determined by the cost-potential price ratio and the efficiency constant, i.e., $X = w_f/qA_f$, whereas the fishery effort settles down on $E_f = \frac{\sigma}{q}(1 - \gamma_6/\gamma_1 - \alpha\psi_e) = \frac{\sigma}{q}(1 - w_f/qKA_f - \alpha\psi_e)$. We notice that since the cost-potential price ratio (w_f/A_f) is fixed in this case, the growth-retardation mechanism has no long run impacts on the fish stock, as long as the strength of the mechanism is below the critical value. However, the temporal evolution is altered. Furthermore, we notice how an increase in the growth-retardation parameter causes a reduced long run harvest volume and thereby lower the fishery effort. From the initial conditions, shown in Fig. 7b, the fishery will be profitable causing a short run increased effort, which in turn leads to a reduced biomass density. A reduced fish stock makes the fishery unprofitable causing a reduction in the effort. The reduced harvest leads to biomass growth, which again leads to an increase in the effort. The biomass and effort variables oscillate and relaxate towards the stable

equilibrium state. An increase in the growth-retardation parameter, will result in a stabilization on a lower level of fishery effort.

In Fig. 8 we have presented an overview of the properties of the equilibrium states of the system (53)–(56) as a function of the growth-retardation parameter α.

(ii) The case with separate price formation.

Next, let us consider the case with separate price formation. This means that we assume that the marginal willingness to pay only depends on the market volume for each of the markets isolated. This parameter regime captures the situation when the harvest volume and the aquaculture production volume do not influence the price of the farmed fish and the price of the harvested fish, respectively. This means that we assume non-existence of cross-market volume mechanisms and that the two different products are independent in demand. By this assumption it follows that $\beta_i > 0$ and $\beta_{ij} = 0$, $(i, j = a, f)$ $(i \neq j)$. In the dimensionless setting this assumption corresponds to $\gamma_4 = \gamma_{10} = 0$. A detailed analysis of the properties of the dynamical system (20)–(29) for this case is presented in Appendix B. Here we only recapitulate the main results. It turns out that the existence and stability theory for the equilibrium states in this case is qualitatively the same as in subcase i) in the present subsubsection, with the existence of boundary equilibrium points of the type $Q_1^{(\pm)}$ and $Q_2^{(\pm)}$ as well as an interior equilibrium point $Q_e^{(\pm)}$. Moreover, two critical growth-retardation parameters $\alpha_\pm^{(2)}$ and $\alpha_\pm^{(1)}$ with $0 < \alpha_\pm^{(2)} < \alpha_\pm^{(1)}$ are detected, hence dividing the α-range into three subintervals. Thus, the existence regimes and the corresponding stability results for the equilibrium points $Q_1^{(\pm)}$, $Q_2^{(\pm)}$ and $Q_e^{(\pm)}$ as functions of the growth-retardation parameter α exhibit qualitatively the same properties as in case i) in the present subsection. The results are also in this case conveniently summarized in Fig. 8.

We finally illustrate the behavior of the dynamical system (20)–(29) for the case $\gamma_4 = \gamma_{10} = 0$ when where the initial condition is chosen in the vicinity of its asymptotically stable equilibrium point. The graphs of the solution to this system are displayed in Fig. 9a and b. The input parameters used in these computations underlying these plots are given as in Table 4, except that we let $\gamma_4 = \gamma_{10} = 0$. We notice that the result presented in Fig. 9b is similar to the findings summarized in Fig. 7b. The only differences consist of the inclusion of the direct market volume impact, with no cross-industry impact present. In Fig. 9b we notice the same type of oscillatory development as in Fig. 7b. However, since the harvest volume influences prices and thereby makes a lower catch volume more valuable in the market, the equilibrium biomass density becomes lower and the effort higher compared to what one obtains in the constant price case. Also in this case we conclude that an increased growth-retardation parameter causes a reduction in the long run fishery effort.

3.3. Existence and stability of interior equilibrium points

3.3.1. Existence of interior equilibrium points

Here we summarize the existence results for equilibrium points where all the coordinates are strictly positive. Such points are hereafter referred to as *interior equilibrium points*. A detailed account of the derivation of these results can be found in Appendix C.

We use here the notation (59) for the interior equilibrium points. According to Appendix C the coordinates ξ_e, θ_e and ψ_e can be expressed in terms of the coordinate η_e:

$$\xi_e = V(\eta_e), \quad \theta_e = U(\eta_e)V^{-1}(\eta_e), \quad \psi_e = \psi_\pm(\eta_e) \tag{60}$$

Here U and V are the rational functions

$$U(\eta_e) = -\gamma_{11}\frac{(\eta_e - \hat{\eta}_-)(\eta_e - \hat{\eta}_+)}{(\eta_e - \eta_-)(\eta_e - \eta_+)}.$$

$$V(\eta_e) = \frac{\gamma_6(U(\eta_e) + \gamma_3)(\eta_e + \gamma_5)}{\gamma_1(U(\eta_e) + \gamma_3)(\eta_e + \gamma_5) + \gamma_2(\eta_e + \gamma_5) + \gamma_4(U(\eta_e) + \gamma_3)},$$

in η_e whereas $\psi_\pm$ are the functions

$$\psi_\pm(\eta_e) \equiv \frac{1}{2\varrho\eta_e}\left[\gamma_{14} \pm \sqrt{\gamma_{14}^2 - 4\varrho^2\gamma_{13}^2\eta_e^2}\right]. \tag{61}$$

In order to ensure the positivity of the coordinates ξ_e and θ_e it is necessary to impose the condition $\eta_e \in J$ where

$$J = (\eta_+, \hat{\eta}_+). \tag{62}$$

Here $\eta_\pm$ is given by

$$\eta_\pm = \frac{1}{2\gamma_{12}}\left(\gamma_7 - \gamma_9\gamma_{12} \pm \sqrt{D}\right)$$

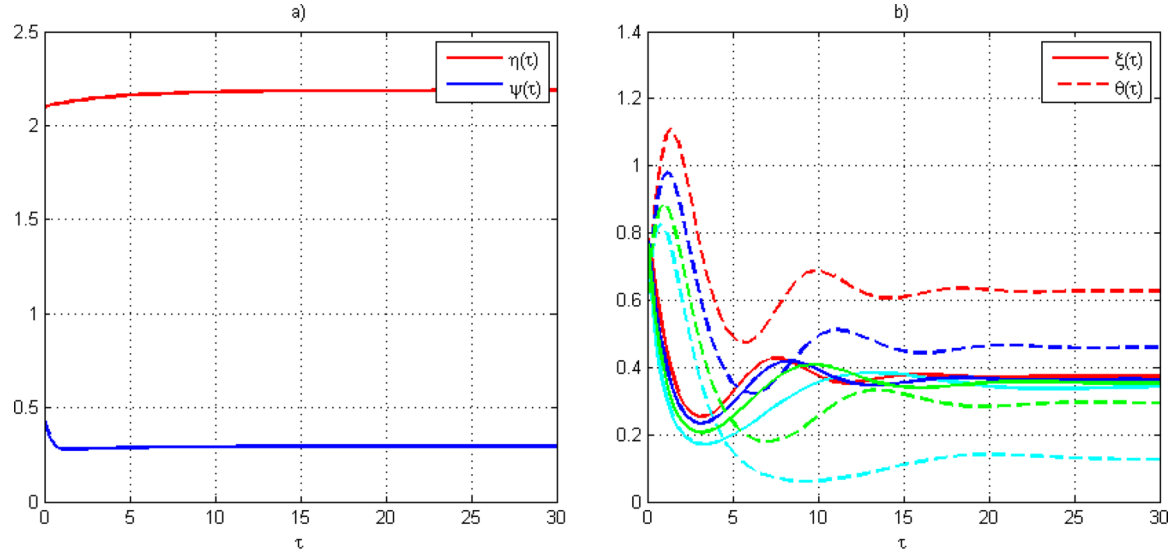

Fig. 9. Numerical example illustrating the behavior of the system (20)–(29) for the case $\gamma_4 = \gamma_{10} = 0$ as a function of the growth-retardation parameter α. Input data in the computations are given in Table 4, except that we let $\gamma_4 = \gamma_{10} = 0$. (2.1861,0.2944) is the asymptotically stable equilibrium state of the 2*D* subsystem (20)–(24), whereas (2.1861,0.8492) is a saddle point. The solution of subsystem (25)–(26) with initial condition $(\eta, \psi) = (2.1, 0.45)$ close to the asymptotically stable equilibrium point is depicted in Fig. 9a. Fig. 9b shows the temporal development of ξ and θ for $\alpha = 0$ (red), $\alpha = 0.6$ (blue), $\alpha = 1.2$ (green) and $\alpha = 1.8$ (turquoise) (corresponding to the points *K, L, M* and *N*, respectively, in Fig. B.13). The function ψ presented by the graph in Fig. 9a acts as an input function. $(\xi, \theta) = (0.8, 0.6)$ is the initial condition for (ξ, θ).

with the discriminant D given as (39). $\hat{\eta}_{\pm}$ is given by(38), respectively. Finally, but not least, the parameters ϱ, γ_{13} and γ_{14} must satisfy the condition (40) in order to guarantee the positivity of the coordinate ψ_e.

In the procedure for determination of the interior equilibrium points we conveniently distinguish between the cases $\alpha = 0$ and $\alpha > 0$.

1. *The case* $\alpha = 0$
   The interior stationary points Q_e are determined by the non-negative solutions of the equation

$$\varphi(\eta_e) = 1, \quad \eta_e \in J. \tag{63}$$

   where φ is defined as

$$\varphi(\eta_e) = V(\eta_e) + U(\eta_e)V^{-1}(\eta_e) \tag{64}$$

   The maximal number of solutions to the Eq. (63) in the interval J defined by (62) for which $\varphi'(\eta_e) \neq 0$ is 7. The change of the number of equilibrium points occurs when the nontransversal intersection conditioned by $\varphi(\eta_e) = 1$, $\varphi'(\eta_e) = 0$ takes place. This typically happens when one of the parameters in the function φ passes through a critical, bifurcation value.
   The procedure for determining the interior equilibrium points Q_e proceeds as follows: We first find all η_e satisfying the Eq. (63). We compute the coordinates ξ_e, θ_e and ψ_e by means of (60). We notice here that each η_e gives rise to two interior equilibrium points through the expression (61).
   Our main result regarding existence of interior equilibrium points can thus be summarized in the following theorem:

Theorem 1. *In the case* $\alpha = 0$, *the system (20)–(29) has at least two interior equilibrium points. The generic situation consists of an even number of interior equilibrium points. The maximal number of such equilibrium points is 14.*

For the input parameters given by Group 2 - Group 4 in Table 4, we find that the numerical solution of (63) is given by $\eta_e = 2.3769$. Now, by following the procedure outlined above, we readily find that the interior equilibrium points denoted by $Q_e^{(-)}$ and $Q_e^{(+)}$ are given as

$$Q_e^{(-)} = (\xi_e, \theta_e, \eta_e, \psi_-) = (0.3626, 0.6374, 2.3769, 0.3629),$$

$$Q_e^{(+)} = (\xi_e, \theta_e, \eta_e, \psi_-) = (0.3626, 0.6374, 2.3769, 0.6889)$$

   when the input parameters are

2. *The case* $\alpha > 0$
   In this case, interior stationary points Q_e are determined by non-negative solutions η_e of the equation

$$\varphi_{\pm}(\eta_e; \alpha) = 1. \tag{65}$$

   where the functions $\varphi_{\pm}: [\eta_+, \hat{\eta}_+] \to \mathbb{R}$ are defined by

$$\varphi_{\pm}(\eta_e; \alpha) \equiv \varphi(\eta_e) + \alpha\psi_{\pm}(\eta_e). \tag{66}$$

   Here the function φ is defined by means of (64). The main result on the interior stationary points Q_e in the case $\alpha > 0$ can be summarized as follows:

Theorem 2. *Assume* $0 < \alpha < \alpha_+^{(2)}$ *where* $\alpha_+^{(2)}$ *is given by*

$$\alpha_{\pm}^{(2)} = \frac{1 - \varphi(\hat{\eta}_+)}{\psi_{\pm}(\hat{\eta}_+)}. \tag{67}$$

and that $\hat{\eta}_+$ *defined by (38)-(39) satisfies the condition (40). Then the system (20)–(29) has at least two equilibrium points of the type* Q_e *in the interior of* Σ_{inv}. *If* $\alpha_+^{(2)} \leq \alpha < \alpha_-^{(2)}$, *the system (20)–(29) has at least one equilibrium solution.*

Based on Theorem 2 we easily arrive at the following uniqueness result:

Corollary 1. *Assume* $0 < \alpha < \alpha_+^{(2)}$ *where* $\alpha_+^{(2)}$ *is given by (67) and that* $\hat{\eta}_+$ *defined by (38)-(39) satisfies the condition (40). Moreover, assume that the functions* $\varphi_{\pm}: (\eta_+, \hat{\eta}_+) \to \mathbb{R}$ *are monotonically decreasing functions. Then the system (20)-(29) has two equilibrium points, denoted by* $Q_e^{(+)}$ *and* $Q_e^{(-)}$ *in the interior of* Σ_{inv}. *If* $\alpha_+^{(2)} \leq \alpha < \alpha_-^{(2)}$, *the system (20)-(29) has one and only equilibrium point* $Q_e^{(-)}$. *For* $\alpha \geq \alpha_-$, *no interior equilibrium points exist.*

For the input parameters listed in Table 4, we find by using the formula (67) that the bounds on α are given as

$$\alpha_-^{(2)} = 1.7402, \quad \alpha_+^{(2)} = 1.0460. \tag{68}$$

consistent with the results in Section 3.2.2. Moreover, by following the computational procedure outlined above we find that the coordinates for the interior equilibrium points $Q_e^{(\pm)}$ emerging from the unique solution of $\varphi_{\pm}(\eta_e; \alpha) = 1$ on the interval $(\eta_+, \hat{\eta}_+]$ are given by

$$Q_e^{(-)} = (0.3435, 0.2813, 2.4004, 0.3752),$$

$$Q_e^{(+)} = (0.3272, 0.0258, 2.4192, 0.6470) \tag{69}$$

for this choice of input parameters and $\alpha = 1$.

A detailed account of the derivation of the results in the present subsection is given in Appendix C.

3.3.2. Stability of interior equilibrium points

The boundary equilibrium point of the type $Q_2^{(-)}$ introduced in Section 3.2.2 is given as

$$Q_2^{(-)} = (0.6123, 0, 2.4212, 0.3877) \tag{70}$$

for the input parameters listed in Table 4 and with $\alpha = 1$. Since $\alpha < \alpha_-^{(2)}$ in this case, this equilibrium point is in accordance with the theory developed in Section 3.2.2 unstable.

In order to assess the stability of the equilibrium point $Q_e^{(-)}$ given by (69) we proceed by computing the Jacobian matrix of the vector field **F** defined by (32) evaluated at this equilibrium point and thereafter determine the eigenvalues of this matrix. This numerical computation gives complex eigenvalues λ_i, $i = 1, 2, 3, 4$ with negative real parts, i.e., $\lambda_1 = -0.1990 + 0.4953i$, $\lambda_2 = -0.1990 - 0.4953i$, $\lambda_3 = -0.1767$, λ_4 thus $= -1.7875$,
showing that $Q_e^{(-)}$ is an asymptotically stable focus. This result is indeed consistent with the small amplitude damped oscillatory behavior about the equilibrium state $Q_e^{(-)}$ summarized in Fig. 10 and in Fig. 11. In Fig. 10 the initial condition is selected in the vicinity of $Q_e^{(-)}$, whereas for Fig. 11 the initial condition is chosen close to the boundary equilibrium point $Q_2^{(-)}$ given as (70). The latter figure shows that $Q_2^{(-)}$ given by means of (70) acts as expected as an repellor in this parameter regime.

The initial value in the fishery effort underlying the computation leading to Fig. 10 is different from the initial value for the computation producing Fig. 11. Fig. 10 describes a situation where this effort is higher than the equilibrium value, while it is just above zero in Fig. 11. This difference leads to different temporal developments in the state variables. In Fig. 10 we observe that the wild fish stock is decreasing in the transient phase as a result of relatively high effort in the harvest activity. For the case demonstrated in Fig. 10 where the effort is relatively low the biomass will increase in the transient phase. The outcome of this makes the fishery more profitable, which causes an increase in the harvesting effort. In both cases we notice the damped oscillatory behavior about the equilibrium state.

We next assess the stability of the interior equilibrium points $Q_e^{(\pm)}$ as a function of the growth-retardation parameter α by fixating the parameters γ_i, $i = 1, 2, \ldots, 14$ and ϱ. The description of this assessment procedure is outlined in Appendix D. We arrive at the following conclusion: For the input parameters in Table 4 we conclude that the equilibrium point $Q_e^{(-)}$ given by (69) is asymptotically stable for all $\alpha \in [0, \alpha_-^{(2)})$, whereas the equilibrium point $Q_e^{(+)}$ is unstable for all $\alpha \in [0, \alpha_+^{(2)})$. Interestingly, we observe that the positive slope condition $R'(\psi_e, \gamma_{13}) > 0$ for the remediation function is fulfilled for $Q_e^{(-)}$, whereas for $Q_e^{(+)}$ we

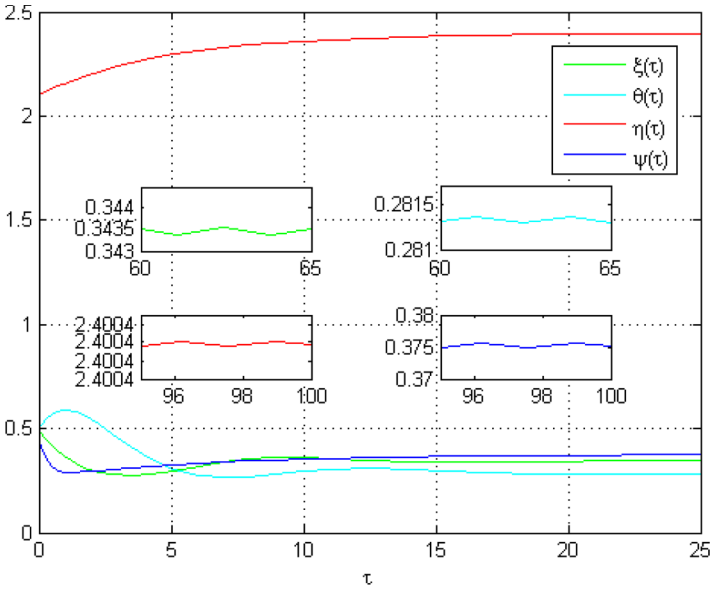

Fig. 10. Numerical example illustrating the behavior of the full system the system (20)–(29). The nondimensional biomass variable ξ (green), the nondimensional effort variable θ (turquoise), the nondimensional effort variable η (red) and the nondimensional accumulated pollution ψ (blue curve) as function of the nondimensional time τ. Input parameters are given in Table 4 and $\alpha = 1$. The initial condition is $(\xi, \theta, \eta, \psi) = (0.5, 0.5, 2.1, 0.45)$, which is close to $Q_e^{(-)}$. The η - and ψ-coordinate of the initial condition should be fixed as in Fig. 3. The insets demonstrate the damped oscillatory nature of the stability.

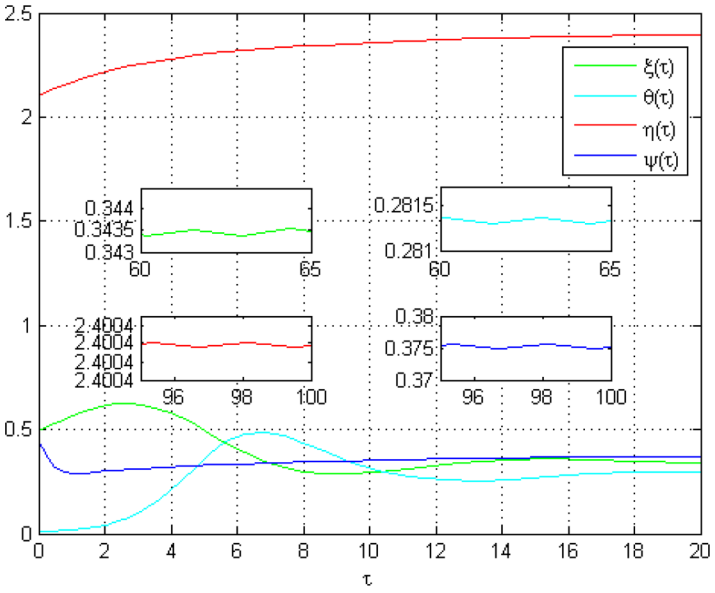

Fig. 11. Numerical example illustrating the behavior of the full system the system (20)–(29). The nondimensional biomass variable ξ (green), the nondimensional effort variable θ (turquoise), the nondimensional effort variable η (red) and the nondimensional accumulated pollution ψ (blue curve) as function of the nondimensional time τ. Input parameters are given in Table 4 and $\alpha = 1$. The initial condition is $(\xi, \theta, \eta, \psi) = (0.5, 0.01, 2.1, 0.45)$, which is close to the unstable boundary equilibrium point $Q_2^{(-)}$ given by (70). The insets demonstrate the damped oscillatory nature of the stability.

have $R'(\psi_e, \gamma_{13}) < 0$ for the input parameters listed in Table 4.

We observe that $\eta_e = \hat{\eta}_+$ is a solution of the system (C.13)–(C.14) when $\alpha = \alpha_{\pm}^{(2)}$. In this limiting case $U(\eta_e) = 0$ from which it follows that $\theta_e = 0$. This means that the equilibrium points $Q_e^{(\pm)}$ merge together with the boundary equilibrium points $Q_2^{(\pm)}$. For $\alpha > \alpha_{\pm}^{(2)}$, we have non-existence of the corresponding interior equilibrium points $Q_e^{(\pm)}$. Cf. Corollary 1. Shoshitaishvilis theorem[8] implies that $Q_e^{(+)}$ is unstable for $\alpha = \alpha_+^{(2)}$. Regarding the relationship between the interior equilibrium point $Q_e^{(-)}$ and the boundary equilibrium point $Q_2^{(-)}$ the following picture thus emerges: The point $Q_e^{(-)}$ is asymptotically stable for $0 \leq \alpha < \alpha_-^{(2)}$ whereas $Q_2^{(-)}$ is unstable in the same parameter regime. For $\alpha = \alpha_2^{(-)}$, $Q_e^{(-)}$ merges together with $Q_2^{(-)}$, and vanishes for $\alpha > \alpha_-^{(2)}$. $Q_2^{(-)}$ is asymptotically stable when $\alpha_-^{(2)} < \alpha < \alpha_-^{(1)}$. The previous stability analysis of $Q_2^{(-)}$ together with the results in this subsection is signalling that a transcritical bifurcation takes place when $\alpha = \alpha_-^{(2)}$. We conclude that the analysis of the existence regimes and the corresponding stability results for the equilibrium points $Q_1^{(\pm)}$, $Q_2^{(\pm)}$ and $Q_e^{(\pm)}$ produces qualitatively the same results as for the special cases investigated in Section 3.2.3. Fig. 8 gives a summary of these results.

Interestingly, the value of $\alpha_-^{(2)}$ given by (68) is less than the numerical values of $\alpha_-^{(2)}$ computed for the two special cases explored in Section 3.2.3. From the viewpoint of bioeconomics this makes sense: For these special cases we have no cross-market impacts. Both market prices are either constant or only influenced by the own industry volume supplied to the consumers. The consequence of this simplification is that an increased aquaculture production will not reduce the profitability in the fishery sector through the price mechanism. Therefore we expect a higher value of the critical growth retardation parameter $\alpha_-^{(2)}$ in these special cases as compared to the general case.

3.3.3. Low aquaculture production effect on the biomass growth ($0 < \alpha \ll 1$)

We want to study the model (7), (8), (16) and (18) in the limit $\alpha \to 0^+$. This means that we assume the effect on biomass growth from aquaculture production to be weak (or negligible). Hence, this case isolates the product market interactions between the two industries. Mathematically speaking, we notice that the right hand side of the 3*D*

[8] See Chapter 6 in Arnold (1988).

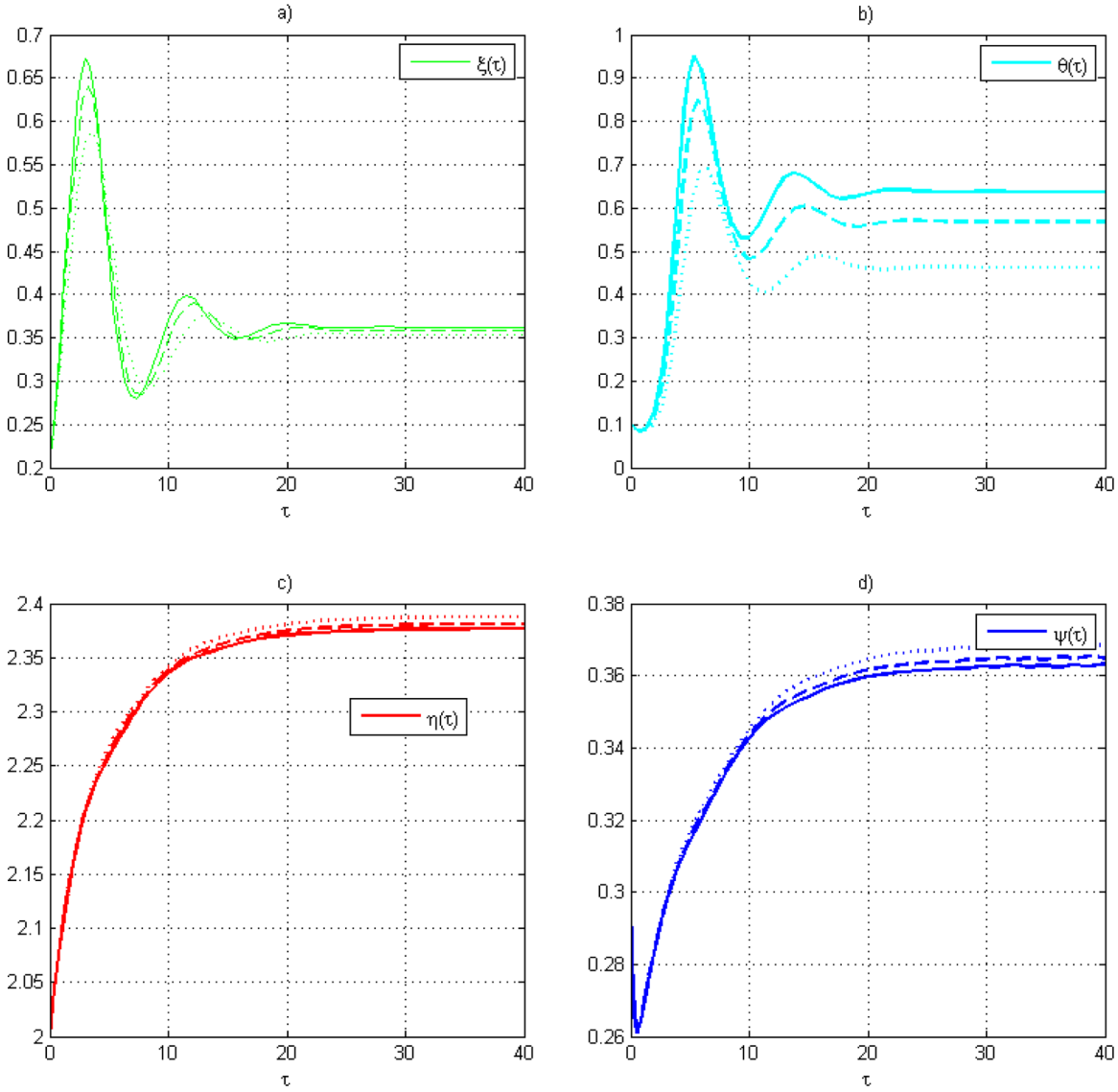

Fig. 12. The temporal evolution of the 4 state variables ξ (green), θ (turquoise), η (red) and ψ (blue) in the regime of low aquaculture production effect on the biomass growth. The input parameters are given in Table 4 with $\alpha = 0$ (solid line), $\alpha = 0.2$ (dashed line) and $\alpha = 0.5$ (dotted line). The initial condition is selected close to the asymptotically stable interior equilibrium point $Q_e^{(-)}$ for $\alpha = 0$.

autonomous subsystem (20)–(22) does not depend on ψ when $\alpha = 0$. Hence, we can analyze this subsystem independently of the pollution Eq. (23) and view the component η as an input function in the latter equation.

In Fig. 12 we demonstrate the effect of weak aquaculture production effect on the biomass growth ($0 < \alpha \ll 1$) numerically. The input parameters are given in Table 4. The initial condition is in the vicinity of the boundary equilibrium point $Q_e^{(-)}$. This figure confirms numerically the asymptotic stability of the interior equilibrium point as well as the predictions of Vasil'eva et al. (1995) with respect to regularly perturbed dynamical systems. See Appendix E for more details.

Fig. 12 describes the case with all biological and economic mechanisms present in our model. In the special case without negative growth impact ($\alpha = 0$) we observe the wellknown oscillatory temporal development. The presence of low and moderate growth-retardation causes a reduced fishery effort and fishery biomass. Unlike the special cases in Figs. 7 and 9, the cross-price effects are present in Fig. 12. As a consequence of this mechanism we notice that increased negative biological externalities will stimulate aquaculture production and accumulated pollution from this industry. This is caused by the cross-price market interaction, where a reduced wild fish volume induces a higher market value for the aquaculture products, and thereby making the aquaculture industry more profitable.

4. Concluding remarks and outlook

As 70% of the Earth's surface is covered by sea, the management of the sea and the coastal zones has become more important. Researchers from different disciplines often use the notion *blue economy* when studying the inter-relations between different marine economic activities. This includes commercial industries and their interplay with physical and ecological systems in coastal zones and the oceans. There will be aquaculture production for feeding the still growing population of the world. A key issue in interdisciplinary marine research is how to achieve an economic sustainable usage of the marine resources. The present contribution is within the auspices of this type of research. We have proposed a conceptual and simplified theoretical model for possible interrelations between two commercial marine activities: aquaculture production, which possibly induces marine pollution, and an industry harvesting a wild fish stock. This model assumes the form of a

nonlinear autonomous dynamical system. We identify and characterize possible equilibrium states within the framework of this system.

4.1. Main results

When investigating the impact pollution from aquaculture has on the growth on the wild fish stock, we found that a necessary (but not sufficient) condition for stability are low and moderate values of the emission remediation parameter. Three intervals of the growth-retardation parameter are identified in this regime of the emission-remediation ratio. The regime of low and negligible influence of the pollution on the biomass evolution gives rise to the existence of an asymptotically stable equilibrium state characterized by a finite biomass and a finite effort in the fishery. In the same regime we identify two unstable equilibrium states of which the former one is characterized by no effort in the fishery, whereas the latter one is characterized by no biomass and no effort. When the growth retardation parameter exceeds a certain threshold, the fishery becomes unprofitable and the equilibrium state characterized by no effort in the fishery becomes asymptotically stable. By a further increase in this parameter above a higher threshold value, also the biomass are wiped out and the equilibrium state characterized by no biomass and no effort becomes asymptotically stable.

Fig. 8 summarizes the findings regarding the existence and stability of equilibrium states as a function of the growth-retardation parameter α. A notable feature is that the structure of this dependence is the same as the one observed for the existence and stability properties of the equilibrium states as a function of the growth-retardation parameter α in the simplified models for fixed prices and separate price formation. The results regarding the existence and stability of the equilibrium states seem to be sensible from a bioeconomic viewpoint. Our findings confirm that when we have a small and moderate biomass growth-retardation effect, the simple bioeconomic effects and the conventional interrelations between the two seafood markets are present. The equilibrium is characterized by activities in both industries. Moreover, when we are in the intermediate value regime of the biomass growth retardation, the harvesting industry becomes unprofitable due to pollution, even in the case with a finite wild fish stock. Finally, for even higher values of the biomass growth-retardation parameter, the model shows that the stable equilibrium state also means that the wild fish stock vanishes. We are not aware of any papers discussing this type of global properties of the retardation impact.

4.2. Possible extensions

Our model is based on several simplifying assumptions. Other possible interesting factors could be relevant when elaborating on the functioning between ecology, marine industries and consumption markets for seafood.

For instance, we have only considered one typical exploited wild fish stock and the consequences of aquaculture production and pollution on the growth potential of that fish stock and the associated product market. We analyze a conceptual model without a specific context. In reality, there are many economic activities in the coastal zone and in the oceans, and pollution stems from many sources related to such production and consumption, not only sea farming. In addition, the effects from emissions can be more complex, and the dynamical structure of the influences on the fisheries could be more sophisticated than in our simple model. Widening the biological focus could reveal different effects on various species that are interrelated in the ecological system, and such an analysis could capture important dynamical aspects of pollution in the fisheries.

Furthermore, applicability of the present modelling framework is limited to problem for which spatial effects can be ignored. In line with this we expect that our model can be useful when dealing with problems for which transport effects can be neglected. This could be the case in closed or strictly coastal ecosystems. On the contrary, physical effects like advection could play a significant role when studying the transport of pollutants and wild fish in for example open ocean ecosystems. A possible extension of the present work could therefore consist of taking into account spatial effects such as advection-diffusion effects, in a way analogous to Heilmann et al. (2018). The diffusion effects describe random movements of the pollutants and the wild fish population, while the advection terms account for the fitness taxis i.e. the preference of both the pollutants and the wild fish for moving towards more favorable regions. This will result in a coupled system of nonlinear partial differential equations of the advection-diffusion type. A further development consists of introducing more biological realism into this modeling framework by taking account of nonlocal diffusion effects and/or encounter probabilities between pollutants and the wild fish, thus ending up with a spatially nonlocal and nonlinear advection-diffusion system. Such systems are generically known for supporting spatial and spatio-temporal patterns, caused by a Turing type of instability. See Heilmann et al. (2018), Murray (2001) and the references therein for more details. The approaches for dealing with actual advection-diffusion systems can also be found in Cosner (2014).

Another possible extension consists of adding time dependent stochastic effects. Quantities in both model blocks are subject to uncertainties, and could because of this be treated as stochastic processes. For example, it would be of interest to model the pollution state producing a maximal remediation capacity as a stochastic variable. This will eventually lead to a modeling framework, which must be dealt with by using the theory of stochastic dynamical systems as elaborated in Øksendal (2003). This problem might be a topic for future research.

Still another possible extensions could consist of taking absolute and/or distributed time lag into account in different parts of the modelling blocks, using the approaches presented in Cushing (2013).

Our analysis presumes that the fishery is characterized by an open access regime. In future investigations one should also focus on environmental and fishery policies. Such policies could be based on maximizing social welfare in a dynamic perspective, i.e., identifying preferred allocations of possible stable equilibrium states of economic growth, size of the fish stock, the effort in harvesting and volume of effort and production of sea farmed fish. Here public regulatory mechanisms can play a crucial role. Such mechanisms could work to limit the emissions impact from aquaculture, or find ways of increasing the remediation capacity. Regulations could take the form of renovation policies, or use indirect means such as taxes and subsidies to bring about a preferable development. Developing the model further by taking into account one or more of the possible complicating aspects mentioned above, is an interesting task for future research in the field of the blue economy, where the primary focus is on aquaculture production, marine pollution and fish harvest. In particular, empirical studies focusing on interrelations between wild fish and aquaculture, based on dynamical modeling, would be needed to decide the relevance of the different equilibria we have studied in our theoretical model.

Declaration of Competing Interest

The authors declare that they have no known competing financial interests or personal relationships that could have appeared to influence the work reported in this paper.

Acknowledgements

The present work was initiated in Spring 2019 when E. Burlakov visited Norwegian University of Life Sciences and Nord University (Bodø), Norway. The authors are grateful to Professor Arcady Ponosov (Faculty of Science and Technology, Norwegian University of Life Sciences) and Professor Mads Peter Sørensen (Technical University of Denmark) for fruitful and stimulating discussions during the

preparation phase of this paper. The authors would also like to thank Senior Research Fellow Eric Nævdal (Frisch Centre, University of Oslo) for constructive remarks and cand. agric. Asbjørn Olafsen for language editing. The authors would also like to thank the reviewers for constructive remarks. This research work was supported by the Norwegian University of Life Sciences and The Research Council of Norway, project number 239070. The work of Evgenii Burlakov was conducted in V.A. Trapeznikov Institute of Control Sciences of RAS (Russian Academy of Sciences) and supported by the Russian Science Foundation (grant no. 20-11-20131).

Appendix A

Fundamental properties of the dynamical system (20)–(29).

The dynamical system (20)–(29) has the following property summarized in the following theorem:

Theorem 3. *Let Φ^τ denote the flow of the dynamical system (20)–(29). The set Σ_{inv} defined by*

$$\Sigma_{inv} = \{(\xi, \theta, \eta, \psi) \in \Sigma;\ \xi \geq 0,\ \theta \geq 0,\ \eta > 0,\ \psi \geq 0\}$$

is an invariant set i.e. $\Phi^\tau(\Sigma_{inv}) \subseteq \Sigma_{inv}$ which means that an orbit starting in Σ_{inv} will remain in Σ_{inv}.

Proof. Introduce the vector field $\mathbf{F}_2$ defined as

$$\mathbf{F}_2(\xi, \theta, \eta, \psi) = \begin{pmatrix} \mathcal{K}(\xi, \theta, \eta, \psi) \\ \mathcal{H}(\xi, \theta, \eta, \psi) \end{pmatrix}.$$

Let $\mathbf{e}_\psi$ and $\mathbf{e}_\eta$ denote the unit vectors along the ψ - and η - axis, respectively. Simple computation reveals that

$$\mathbf{F}_2(\xi, \theta, \eta, 0)\cdot\mathbf{e}_\psi = \varrho\eta > 0 \quad \text{on the positive } \eta\text{-axis}$$

$$\mathbf{F}_2(\xi, \theta, \eta, \psi)\cdot\mathbf{e}_\eta = H(\xi, \theta, \eta, \psi).$$

We notice that H is singular for points located at the hyperplane $\eta = 0$. This means that no orbits of the system (20)–(29) can cross this hyperplane. We conclude that solutions of the 2D subsystem $\frac{d\psi}{d\tau} = \mathcal{K}$, $\frac{d\eta}{d\tau} = \mathcal{H}$ starting in the first quadrant of the ψ, η - plane will remain in that quadrant. Here we tacitly view ξ and θ as given functions of τ.

Next, let us consider the subsystem (20)–(21). This subsystem is of the Lotka-Volterra type. Then, by appealing to Lemma 2 in Appendix B in Bergland et al. (2019), we conclude that $\xi(0) > 0$ ($\theta(0) > 0$) if and only if $\xi(\tau) > 0$ ($\theta(\tau) > 0$) and $\xi(0) = 0$ ($\theta(0) = 0$) if and only if $\xi(\tau) = 0$ ($\theta(\tau) = 0$) for $\tau > 0$.

Hence, we can conclude that any solution of the full system (20)–(23) with initial condition in Σ_{inv} remains in Σ_{inv}. □

Appendix B

The analysis of case with separate price formation in the markets.

The dynamical system (20)–(29) simplifies to

$$\frac{d\xi}{d\tau} = \xi(1 - \xi - \theta - \alpha\psi), \tag{B.1}$$

$$\frac{d\theta}{d\tau} = \theta\left[\left(\gamma_1 + \frac{\gamma_2}{\xi\theta + \gamma_3}\right)\xi - \gamma_6\right], \tag{B.2}$$

$$\frac{d\eta}{d\tau} = f_2(\eta; \eta_\pm), \tag{B.3}$$

$$\frac{d\psi}{d\tau} = \varrho\eta - \gamma_{14}R(\psi; \gamma_{13}). \tag{B.4}$$

when $\gamma_4 = \gamma_{10} = 0$. Here

$$f_2(\eta; \eta_\pm) \equiv -\frac{\gamma_{12}}{\eta^2(\eta + \gamma_9)}(\eta - \eta_-)(\eta - \eta_+). \tag{B.5}$$

and

$$\eta_\pm = \frac{1}{2\gamma_{12}}\left(\gamma_7 - \gamma_9\gamma_{12} \pm \sqrt{D}\right) \tag{B.6}$$

with the discriminant D given as (39). We use the same approach as in the case with constant product prices: We readily find boundary equilibrium points of the type $Q_1^{(\pm)}$ and $Q_2^{(\pm)}$, i.e.,

$$Q_1^{(\pm)} = (0, 0, \eta_e, \psi_e), \tag{B.7}$$

$$Q_2^{(\pm)} = (\psi_\pm(\alpha_\pm^{(1)} - \alpha), 0, \eta_e, \psi_\pm), \quad \alpha_\pm^{(1)} = 1/\psi_\pm, \quad 0 \leq \alpha < \alpha_\pm^{(1)}, \tag{B.8}$$

where $\eta = \eta_e = \eta_+$ whereas $\psi_e = \psi_\pm$ is given as (34) with $\eta = \eta_+$, i.e.,

$$\psi_{\pm} \equiv \frac{1}{2\varrho\eta_+}\left[\gamma_{14} \pm \sqrt{\gamma_{14}^2 - 4\varrho^2\gamma_{13}^2\eta_+^2}\right].$$

Here we have tacitly assumed that $0 < \eta_+ < \frac{\gamma_{14}}{2\varrho\gamma_{13}}$ to ensure $\psi_{\pm}$ to be real (and positive). We notice that the boundary equilibrium points $Q_1^{(\pm)}$ and $Q_2^{(\pm)}$ investigated in Sections 3.2.1 and 3.2.2, respectively, deform to the equilibrium points (B.7) and (B.8) when $\gamma_4, \gamma_{10} \to 0^{(+)}$. The stability results for $Q_1^{(\pm)}$ and $Q_2^{(\pm)}$ given by (B.7) and (B.8) are qualitatively the same as the results derived in Sections 3.2.1 and 3.2.2: $Q_1^{(+)}$ and $Q_1^{(+)}$ are unstable. $Q_1^{(-)}$ is asymptotically stable for $\alpha > \alpha_-^{(1)}$ and unstable for $0 \le \alpha < \alpha_-^{(1)}$, whereas $Q_2^{(-)}$ is asymptotically stable for $\alpha_-^{(2)} < \alpha < \alpha_-^{(1)}$ and unstable for $0 \le \alpha < \alpha_-^{(2)}$. The equilibrium, states $Q_2^{(\pm)}$ merge together with $Q_1^{(\pm)}$ for $\alpha = \alpha_{\pm}^{(1)}$ and cease to exist for $\alpha > \alpha_{\pm}^{(1)}$. We have a transcritical bifurcation for $\alpha = \alpha_-^{(1)}$.

Next, let us study existence and stability of interior equilibrium points $Q_e^{(\pm)} = (\xi_e, \theta_e, \eta_e, \psi_e)$. We first observe that $\eta_e = \eta_+$, and consequently that $\psi_e = \psi_{\pm}$ where $\psi_{\pm}$ is given as (34) with $\eta = \eta_+$. The conditions $\mathcal{F}(\xi, \theta, \eta, \psi) = 0$, $\mathcal{G}(\xi, \theta, \eta, \psi) = 0$ can now be written as

$$\xi + \theta = \mu_e, \tag{B.9}$$

$$\left[\gamma_1 + \frac{\gamma_2}{\xi\theta + \gamma_3}\right]\xi - \gamma_6 = 0 \tag{B.10}$$

where μ_e is defined by

$$\mu_e \equiv 1 - \alpha\psi_e. \tag{B.11}$$

We readily observe that a necessary condition for having strictly positive solutions of this system of equations is given by $0 \le \alpha < \alpha_e$ where $\alpha_e \equiv 1/\psi_e$. This restriction imposed on α implies that $0 < \mu_e \le 1$. Moreover, we must impose the condition that $0 < \xi, \theta < \mu_e$. From the last equation in this hierarchy, we find that

$$\theta = \frac{\gamma_2}{\gamma_6 - \gamma_1\xi} - \frac{\gamma_3}{\xi} = \frac{(\gamma_2 + \gamma_1\gamma_3)\xi - \gamma_3\gamma_6}{\xi(\gamma_6 - \gamma_1\xi)}. \tag{B.12}$$

Then by inserting this expression into the first equation we readily find that, ξ satisfies the cubic equation

$$\mathcal{P}_3(\xi, \mu_e) = 0 \tag{B.13}$$

where $\mathcal{P}_3$ is the cubic polynomial

$$\mathcal{P}_3(\xi, \mu_e) \equiv \gamma_1\xi^3 - (\gamma_6 + \mu_e\gamma_1)\xi^2 + (\mu_e\gamma_6 - \gamma_2 - \gamma_1\gamma_3)\xi + \gamma_3\gamma_6 \tag{B.14}$$

in ξ, parameterized by means of μ_e. Simple analysis reveals that

$$\lim_{\xi\to\pm\infty} \mathcal{P}_3(\xi, \mu_e) = \pm\infty, \quad \mathcal{P}_3(0, \mu_e) = \gamma_3\gamma_6 > 0, \tag{B.15}$$

$$\mathcal{P}_3(\mu_e, \mu_e) = (\gamma_1\gamma_3 + \gamma_2)(\mu_e^* - \mu_e), \quad \mu_e^* \equiv \frac{1}{\frac{\gamma_1}{\gamma_6} + \frac{\gamma_2}{\gamma_3\gamma_6}} < 1, \tag{B.16}$$

$$\mathcal{P}_3'(\mu_e, \mu_e) = \gamma_1\mu_e(\mu_e - \frac{\gamma_6}{\gamma_1}) - \gamma_2 - \gamma_1\gamma_3. \tag{B.17}$$

Moreover, $\mathcal{P}_3$ always has extremal points of which one is always positive. In fact, we find that

$$\xi_m(\mu_e) = \frac{1}{3\gamma_1}\left[\gamma_6 + \mu_e\gamma_1 + \sqrt{(\gamma_6 - \frac{1}{2}\gamma_1\mu_e)^2 + \frac{3}{4}\gamma_1^2\mu_e^2 + 3\gamma_1(\gamma_2 + \gamma_1\gamma_3)}\right] > 0$$

is a strictly positive local minimum point of $\mathcal{P}_3$. Since $\mu_e^* < \frac{\gamma_6}{\gamma_1}$, we arrive at the following conclusions: For $\mu_e < \mu^*$, we get $\mathcal{P}_3(\mu_e, \mu_e) > 0 > \mathcal{P}_3'(\mu_e, \mu_e)$ from which it follows that $\mathcal{P}_3$ has no positive zeros in the interval $(0, \mu_e)$. In the complementary regime $\mu_e^* < \mu_e \le 1$, we find that $\mathcal{P}_3(\mu_e, \mu_e) < 0$. In this case we conclude that $\mathcal{P}_3$ has one and only positive zero, say $\xi_1 = \xi_1(\mu_e)$, for which $\xi_1(\mu_e) < \mu_e$. For the transition value $\mu_e = \mu_e^*$, we readily find that $\xi_1(\mu_e^*) = \mu_e^*$. By appealing to (B.11), (B.16) and (52) (with $\gamma_4 = 0$), we conclude that there is a unique interior equilibrium point for $0 \le \alpha < \alpha_{\pm}^{(2)}$, whereas for $\alpha > \alpha_{\pm}^{(2)}$ no such equilibrium point exists.

The result of this analysis is summarized in Fig. B.13. The input parameters underlying this computation are given in Table 4, except that we let $\gamma_4 = \gamma_{10} = 0$. $\psi_e = \psi_- = 0.2944$ is the ψ - coordinate of the asymptotically stable equilibrium point of the subsystem (B.3)–(B.4). μ_e^* defined by (B.16) is given as $\mu_e^* = 0.3333$. It corresponds to $\alpha_-^{(2)} = 2.2644$ through the definition (B.11). The ξ - values of the points marked with *K, L, M* and *N* are ξ - coordinates of four different interior equilibrium points of the system (B.1)–(B.4) for different values of $\alpha = 0$, $\alpha = 0.6$, $\alpha = 1.2$ and $\alpha = 1.8$, respectively. Notice that these four α - values produce the four graphs in Fig. 9b.

Finally, we study the stability problem for the case when $\gamma_4 = \gamma_{10} = 0$. Let Q_e denote an interior equilibrium point. The stability of the equilibrium point depends sensitively on the slope of the remediation function evaluated at $\psi = \psi_e$: Q_e is asymptotically stable, if the positive slope condition $R'(\psi_e, \gamma_{13}) > 0$ is fulfilled, whereas it is unstable if $R'(\psi_e, \gamma_{13}) < 0$. This means that the points *K, L, M* and *N* in the graph displayed in Fig. B.13 correspond to asymptotically stable equilibrium points of the system (B.1)–(B.4).

We finally notice that when $\alpha = \alpha_{\pm}^{(2)}$ (corresponding to $\mu_e = \mu_e^*$), $\theta_e \to 0^+$, i.e. which means that the equilibrium states $Q_e^{(\pm)}$ merge together with the boundary equilibrium points of the type $Q_2^{(\pm)}$.

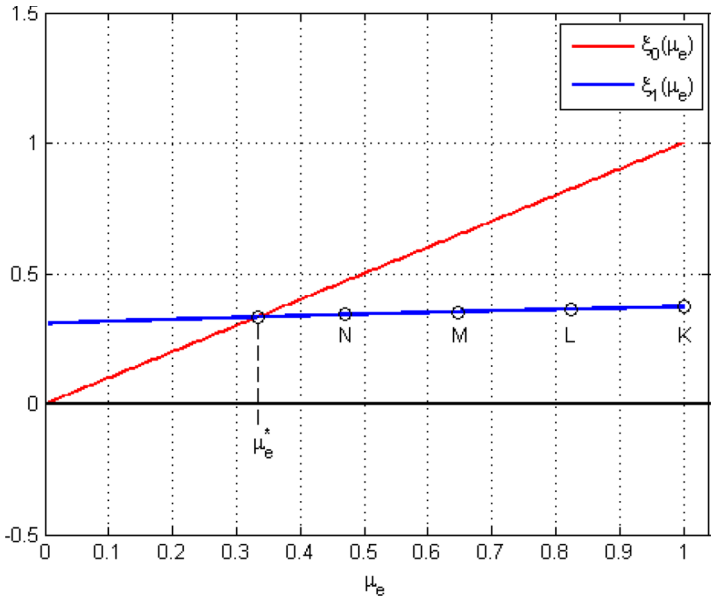

Fig. B1. The graphs of the two functions $\xi = \xi_0(\mu_e) = \mu_e$ and $\xi = \xi_1(\mu_e)$ on the interval (0,1] as functions of $\mu_e = 1 - \alpha\psi_e$. $\xi = \xi_1(\mu_e)$ and $\xi = \xi_2(\mu_e)$ are strictly positive zeros of the polynomial $\mathcal{P}_3$ defined by (B.14). Input parameters in the computations are given in Table 4, except that we let $\gamma_4 = \gamma_{10} = 0$. $\psi_e = \underline{\psi}_- = 0.2944$ is the ψ - coordinate of the asymptotically stable equilibrium point of the subsystem (B.3) - (B.4). μ_e^* defined by (B.16) is given as $\mu_e^* = 0.3333$. It corresponds to $\underline{\alpha}_-^{(2)} = 2.2644$ through the definition (B.11). The ξ - values of the points marked with *K, L, M* and *N* are ξ - coordinates of four different interior equilibrium points of the system (B.1) - (B.4) for different values of $\alpha = 0$, $\alpha = 0.6$, $\alpha = 1.2$ and $\alpha = 1.8$, respectively. Notice that these four α - values are labeling to the four graphs in Fig. 9b.

Table 4
Group 2 - Group 4 parameters used in some numerical examples in the present paper.

Input parameters	
Group 2:	$\gamma_1 = 2$, $\gamma_2 = 0.5$, $\gamma_3 = 0.5$, $\gamma_4 = 0.25$, $\gamma_5 = 1$, $\gamma_6 = 1$
Group 3:	$\gamma_7 = 2$, $\gamma_8 = 0.5$, $\gamma_9 = 0.5$, $\gamma_{10} = 0.25$, $\gamma_{11} = 1$, $\gamma_{12} = 1$
Group 4:	$\gamma_{13} = 0.5$, $\gamma_{14} = 2.5$, $\varrho = 1$

Table 5
The number of positive solutions of the Eq. (33) in different parameter regimes.

Parameter regime	The number of positive solutions of the Eq. (33)
$0 < \eta < \frac{\gamma_{14}}{2\varrho\gamma_{13}}$	2
$\eta = \frac{\gamma_{14}}{2\varrho\gamma_{13}}$	1
$\eta > \frac{\gamma_{14}}{2\varrho\gamma_{13}}$	0

Appendix C

Existence of interior equilibrium points.

Here we detail the procedure in Section 3.3.1 for the detection of interior equilibrium points of the type (59).

We first show that ξ_e and θ_e can be expressed in terms of η_e. The condition $\mathcal{H}(\xi_e, \theta_e, \eta_e, \psi_e) = 0$ enables us to express $\xi_e\theta_e$ as a function of η_e i.e.

$$\xi_e\theta_e = U(\eta_e). \tag{C.1}$$

Here U_e is the rational function

$$U(\eta_e) = -\gamma_{11}\frac{(\eta_e - \hat{\eta}_-)(\eta_e - \hat{\eta}_+)}{(\eta_e - \eta_-)(\eta_e - \eta_+)} \tag{C.2}$$

where

$$\eta_\pm = \frac{1}{2\gamma_{12}}\left(\gamma_7 - \gamma_9\gamma_{12} \pm \sqrt{D}\right) \tag{C.3}$$

whereas $\hat{\eta}_\pm$ is given by (38). The discriminant D is given as (39). We notice that $\eta_- < 0 < \eta_+$, $\hat{\eta}_- < 0 < \hat{\eta}_+$ and $\eta_+ < \hat{\eta}_+$. For the Group 3 parameters

listed in Table 4, we find that $\eta_- = -0.6861$, $\eta_+ = 2.1861$, $\hat{\eta}_- = -0.6712$ and $\hat{\eta}_+ = 2.4212$.

We conclude that the condition $U(\eta_e) > 0$ is fulfilled if $\eta_e \in J$ where J is the open interval

$$J = (\eta_+, \hat{\eta}_+). \tag{C.4}$$

Simple computation reveals that $U'(\eta_e) < 0$.

The condition $\mathcal{G}(\xi_e, \theta_e, \eta_e, \psi_e) = 0$ with (C.1) makes it possible to determine ξ_e as a function of η_e. We readily find that

$$\xi_e = V(\eta_e). \tag{C.5}$$

where the function V is given as

$$V(\eta_e) = \frac{\gamma_6(U(\eta_e) + \gamma_3)(\eta_e + \gamma_5)}{\gamma_1(U(\eta_e) + \gamma_3)(\eta_e + \gamma_5) + \gamma_2(\eta_e + \gamma_5) + \gamma_4(U(\eta_e) + \gamma_3)}. \tag{C.6}$$

Fig. C.14 shows the graphs of the functions U and V defined by (C.2) and (C.6), respectively.

Finally, we find from (C.1) and (C.5) that

$$\theta_e = U(\eta_e)V^{-1}(\eta_e). \tag{C.7}$$

The next step of the analysis of the existence of equilibrium points of the type Q_e proceeds as follows: Let φ be the function

$$\varphi(\eta_e) = \xi_e + \theta_e = V(\eta_e) + U(\eta_e)V^{-1}(\eta_e) \tag{C.8}$$

where U and V are defined by (C.1) and (C.6), respectively. The function $\varphi: (\eta_+, \hat{\eta}_+] \to (0, +\infty)$ is a smooth and positive function for which the properties

$$\lim_{\eta_e \to \eta_+^{(+)}} \varphi(\eta_e) = +\infty, \tag{C.9}$$

$$\varphi(\hat{\eta}_+) = V(\hat{\eta}_+) = \frac{1}{\frac{\gamma_1}{\gamma_6} + \frac{\gamma_2}{\gamma_3\gamma_6} + \frac{\gamma_4}{\gamma_6(\hat{\eta}_+ + \gamma_5)}} \tag{C.10}$$

hold true. The profitability condition (14) (which is equivalent with the inequality (31)) implies that

$$\varphi(\hat{\eta}_+) < 1. \tag{C.11}$$

In the remaining part of the procedure for determination of the interior equilibrium points we distinguish between the cases $\alpha = 0$ and $\alpha > 0$.

1. *The case* $\alpha = 0$

   By inserting (C.5) and (C.7) into the equation $\mathcal{F}(\xi_e, \theta_e, \eta_e, \psi_e) = 1 - \xi_e - \theta_e = 0$, we obtain

   $$\varphi(\eta_e) = 1. \tag{C.12}$$

   The conditions (C.9)–(C.11) imply that the Eq. (C.12) has at least one solution on the open interval $J = (\eta_+, \hat{\eta}_+)$. Moreover, for the case $\varphi'(\eta_e) \neq 0$, the Eq. (C.12) has a an odd number of solutions in this interval. As the Eq. (C.12) can be recasted into a 8th degree polynomial equation, we conclude that the maximal number of solutions to the Eq. (C.12) in the interval J for which $\varphi'(\eta_e) \neq 0$ is 7. The change of the number of equilibrium points takes place when the nontransversal intersection $\varphi(\eta_e) = 1$, $\varphi'(\eta_e) = 0$. The actual findings are summarized as Theorem 2. Fig. C.15 shows the graph of the function φ defined by (C.8) when the input parameters are given by Group 2 and Group 3 in Table 4. In this case the function φ is strictly decreasing on the interval $(\eta_+, \hat{\eta}_+]$, thus showing that the Eq. (63) has a unique solution on that interval.

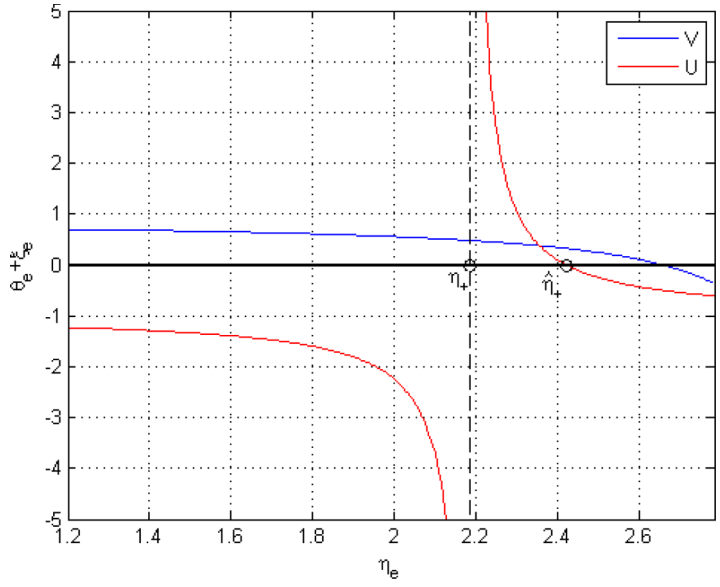

Fig. C1. The graphs of the functions U and V defined by (C.2) and (C.6), respectively. The input parameters are given by Group 2 and Group 3 in Table 4.

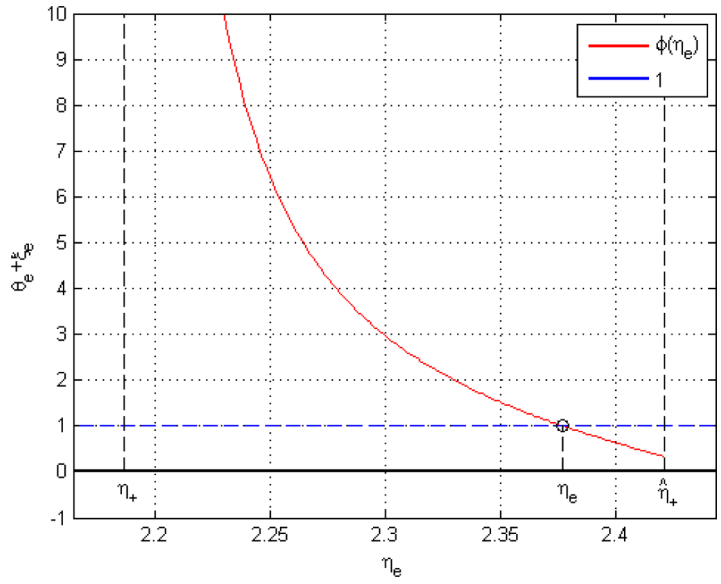

Fig. C2. The graph of the function φ defined by (C.8). The input parameters are given by Group 2 and Group 3 in Table 4.

2. *The case* $\alpha > 0$

The condition $\mathcal{K}(\xi, \theta, \eta, \psi) = 0$ yields (61). Then, by combining this result with the condition $\mathcal{F}(\xi_e, \theta_e, \eta_e, \psi_e) = 0$, we readily find that η_e satisfies the equation

$$\varphi_{\pm}(\eta_e; \alpha) = 1. \tag{C.13}$$

where the function $\varphi_{\pm}: [\eta_+, \hat{\eta}_+] \to \mathbb{R}$ is defined by

$$\varphi_{\pm}(\eta_e; \alpha) \equiv \varphi(\eta_e) + \alpha\psi_{\pm}(\eta_e). \tag{C.14}$$

Here the function φ is defined by means of (C.8). We tacitly assume that the condition (40) is fulfilled in order to ensure that the functions $\psi_{\pm}$ are realvalued (and positive) on the interval $[\eta_+, \hat{\eta}_+]$. Since $\varphi(\hat{\eta}_+) < 1$ and $0 < \psi_{\pm}(\hat{\eta}_+) < +\infty$, we find that $\varphi_{\pm}(\hat{\eta}_+; \alpha)$ is bounded for finite α. Moreover, we observe that the functions $\varphi_{\pm}$ are continuous with respect to α. We therefore conclude that

$$\varphi_{\pm}(\hat{\eta}_+; \alpha) = \varphi(\hat{\eta}_+) + \alpha\psi_{\pm}(\hat{\eta}_+) < 1 \tag{C.15}$$

for $0 \le \alpha < \alpha_{\pm}^{(2)}$. Here we have used the fact that $\alpha_{\pm}^{(2)}$ defined by (52) can be expressed as

$$\alpha_{\pm}^{(2)} = \frac{1 - \varphi(\hat{\eta}_+)}{\psi_{\pm}(\hat{\eta}_+)}. \tag{C.16}$$

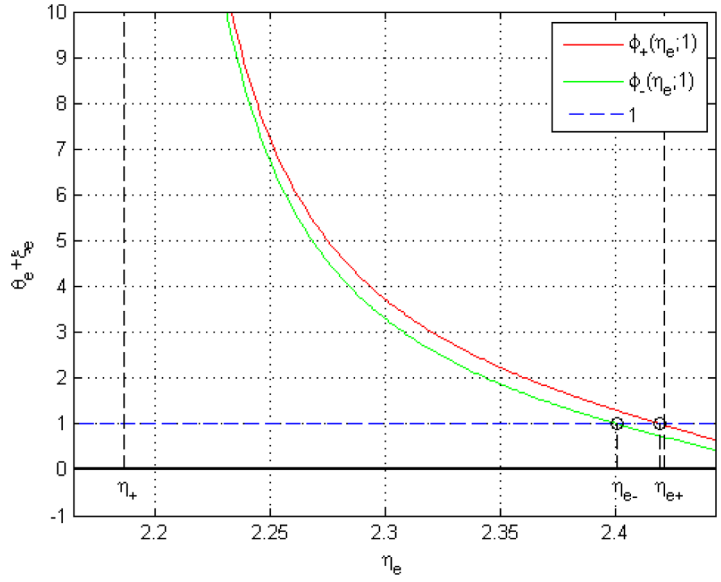

Fig. C3. The graph of the functions $\varphi_{\pm}$ defined by (C.14). The input parameters are given by Table 4 and $\alpha = 1$.

By appealing to the condition (C.9) and the boundedness of $\psi_{\pm}(\eta_+)$, we find that

$$\lim_{\eta_e \to \eta_+^-} \varphi_{\pm}(\eta_e; \alpha) = +\infty \tag{C.17}$$

for all α. We then make use of the continuity of $\varphi_{\pm}$ with respect to η_e to conclude that the equations in (C.13) have at least one solution in the interval $J = (\eta_+, \hat{\eta}_+)$ for $0 \leq \alpha < \alpha_{\pm}^{(2)}$[9]. We recall that $\alpha_+^{(2)} < \alpha_-^{(2)}$. Hence for $0 \leq \alpha < \alpha_+^{(2)}$ we are guaranteed at least one solution of each of the equations $\varphi_+(\eta_e; \alpha) = 1$ and $\varphi_-(\eta_e; \alpha) = 1$, whereas for $\alpha_+^{(2)} \leq \alpha < \alpha_-^{(2)}$ we can only conclude that $\varphi_-(\eta_e; \alpha) = 1$ has at least one solution. We have thus proved Theorem 2.

The content of Theorem 2 and Corollary 1 is visualized in Fig. C.16.

Remark 1. The functions $\varphi_{\pm}: (\eta_+, \hat{\eta}_+) \to \mathbb{R}$ depend continuously on the input parameters in Group 2 - Group 4. This means that the monotonicity property for these functions visualized in Fig. C.16 also holds true for some open neighborhood in the parameter space about the input parameters used in the computations underlying this figure. We suspect that this property holds true in general. An investigation of this problem will, however, lead to cumbersome calculations. We have therefore decided not to pursue this problem in detail, but rather list it is as an open problem.

Appendix D

Stability of interior equilibrium points.

Here we present the procedure for assessing the stability of the interior equilibrium points $Q_e^{(\pm)}$ as a function of α. This means that we fixate the parameters γ_i, $i = 1, 2, ..., 14$ and ϱ whereas we let the growth-retardation parameter α vary.

We first derive the formal expression for the Jacobian $\mathbb{J}_4^{(\alpha)}(Q_e^{(\pm)})$ of the vector field $\mathbf{F}$ defined by (32) evaluated at this equilibrium. Doing this we readily find that it can be written as

$$\mathbb{J}_4^{(\alpha)}(Q_e^{(\pm)}) = \begin{pmatrix} -\xi_e & -\xi_e & 0 & -\alpha\xi_e \\ \theta_e \frac{\partial \mathcal{G}}{\partial \xi}(Q_e^{(\pm)}) & \theta_e \frac{\partial \mathcal{G}}{\partial \theta}(Q_e^{(\pm)}) & \theta_e \frac{\partial \mathcal{G}}{\partial \eta}(Q_e^{(\pm)}) & 0 \\ \frac{\partial \mathcal{H}}{\partial \xi}(Q_e^{(\pm)}) & \frac{\partial \mathcal{H}}{\partial \theta}(Q_e^{(\pm)}) & \frac{\partial \mathcal{H}}{\partial \eta}(Q_e^{(\pm)}) & 0 \\ 0 & 0 & \varrho & -\gamma_{14} R'(\psi_e; \gamma_{13}) \end{pmatrix}. \tag{D.1}$$

Here the partial derivatives $\frac{\partial \mathcal{G}}{\partial \xi}(Q_e^{(\pm)})$, $\frac{\partial \mathcal{G}}{\partial \theta}(Q_e^{(\pm)})$, $\frac{\partial \mathcal{G}}{\partial \eta}(Q_e^{(\pm)})$, $\frac{\partial \mathcal{H}}{\partial \xi}(Q_e^{(\pm)})$, $\frac{\partial \mathcal{H}}{\partial \theta}(Q_e^{(\pm)})$ and $\frac{\partial \mathcal{H}}{\partial \eta}(Q_e^{(\pm)})$ are given as

$$\frac{\partial \mathcal{G}}{\partial \xi}(Q_e^{(\pm)}) = \gamma_1 + \frac{\gamma_4}{\eta_e + \gamma_5} + \frac{\gamma_2 \gamma_3}{(\xi_e \theta_e + \gamma_3)^2},$$

$$\frac{\partial \mathcal{G}}{\partial \theta}(Q_e^{(\pm)}) = -\frac{\gamma_2 \xi_e^2}{(\xi_e \theta_e + \gamma_3)^2},$$

$$\frac{\partial \mathcal{G}}{\partial \eta}(Q_e^{(\pm)}) = -\frac{\gamma_4 \xi_e}{(\eta_e + \gamma_5)^2},$$

$$\frac{\partial \mathcal{H}}{\partial \xi}(Q_e^{(\pm)}) = -\frac{\gamma_{10} \theta_e}{(\xi_e \theta_e + \gamma_{11})^2} \eta_e^{-2},$$

$$\frac{\partial \mathcal{H}}{\partial \theta}(Q_e^{(\pm)}) = -\frac{\gamma_{10} \xi_e}{(\xi_e \theta_e + \gamma_{11})^2} \eta_e^{-2},$$

$$\frac{\partial \mathcal{H}}{\partial \eta}(Q_e^{(\pm)}) = -\left(\frac{\gamma_8}{(\eta_e + \gamma_9)^2} + \gamma_{12}\right) \eta_e^{-2}.$$

In the process of deriving the expressions for these partial derivatives we have made use of the equilibrium conditions $\mathcal{G} = 0$ and $\mathcal{H} = 0$. Moreover, for convenience we have used the notation $Q_e^{(\pm)} = (\xi_e, \theta_e, \eta_e, \psi_e)$.

The characteristic polynomial $\mathcal{P}_{4,\pm}^{(\alpha)}$ of the Jacobian $\mathbb{J}_4^{(\alpha)}(Q_e^{(\pm)})$ which for each $\alpha \in [0, \alpha_{\pm})$ is defined as

$$\mathcal{P}_{4,\pm}^{(\alpha)}(\lambda) = det\{\lambda \mathbb{I}_4 - \mathbb{J}_4^{(\alpha)}(Q_e^{(\pm)})\} \tag{D.2}$$

is a quartic polynomial in λ.

The coefficients of this polynomial are smooth functions of α. Noticing that the constant term $a_4^{(\pm)}$ of this polynomial is equal to $det\{\mathbb{J}_4^{(\alpha)}(Q_e^{(\pm)})\}$. Therefore we can conclude that the corresponding interior equilibrium point is unstable for α for which $det\{\mathbb{J}_4^{(\alpha)}(Q_e^{(\pm)})\} < 0$. In the complementary α - regime we must resort on the Routh-Hurwitz criterion for a quartic polynomial as described in Appendix F in order to assess the stability. We proceed as follows: The stability analysis is based on the Routh - Hurwitz determinants $D_1^{(\pm)}$, $D_2^{(\pm)}$, $D_3^{(\pm)}$ and $D_4^{(\pm)}$ defined in Appendix F. These determinants are smooth functions of α. Noticing that $D_1^{(\pm)}(\alpha) = -tr\{\mathbb{J}_4^{(\alpha)}(Q_e^{(\pm)})\} > 0$, the stability assessment procedure is summarized in the study of the composite map

[9] Notice that this result does not exclude the possibility for the equations in the system (C.13)–(C.14) to have solutions for the complementary α - regime. We do not pursue a study of this problem here, however.

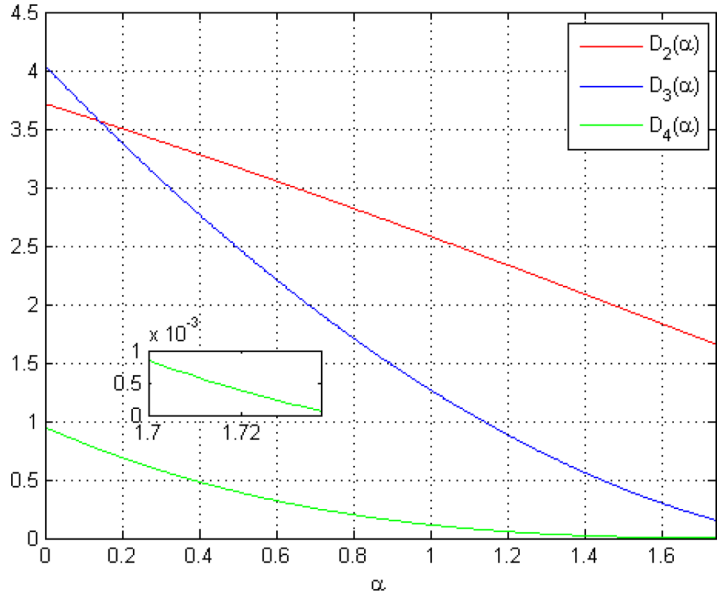

Fig. D1. The Routh-Hurwitz determinants $D_2^{(-)}$, $D_3^{(-)}$ and $D_4^{(-)}$ for the characteristic polynomial $\mathcal{P}_{4,-}^{(\alpha)}(\lambda)$ for the equilibrium point $Q_e^{(-)}$. The input parameters are listed in Table 4. The inset shows that $D_4^{(-)}(\alpha) > 0$.

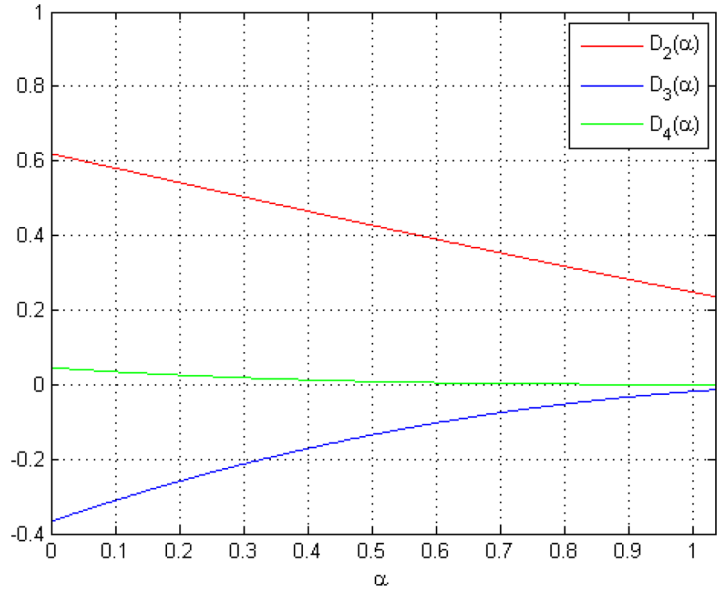

Fig. D2. The Routh-Hurwitz determinants $D_2^{(+)}$, $D_3^{(+)}$ and $D_4^{(+)}$ for the characteristic polynomial $\mathcal{P}_{4,+}^{(\alpha)}(\lambda)$ for the equilibrium point $Q_e^{(+)}$.

$$\alpha \in [0, \alpha_{\pm}^{(2)}) \overset{(D.1)}{\mapsto} \mathbb{J}_4^{(\alpha)}(Q_e^{(\pm)}) \overset{(D.2)}{\mapsto} \mathcal{P}_{4,\pm}^{(\alpha)}(\lambda)$$
$$\overset{(F.2)}{\mapsto} (D_2^{(\pm)}(\alpha), D_3^{(\pm)}(\alpha), D_4^{(\pm)}(\alpha)) \tag{D.3}$$

The composite map (D.3) thus defines a parameterized curve in the $D_2^{(\pm)}$, $D_3^{(\pm)}$, $D_4^{(\pm)}$ - space where $\alpha \in [0, \alpha_{\pm}^{(2)})$. The Routh - Hurwitz criterion implies that we have an α-value, say $\alpha = \alpha_0$, producing a point in the interior of the first octant of this space if and only if the real part of all the zeros of the characteristic polynomial $\mathcal{P}_{4,\pm}^{(\alpha_0)}$ is strictly negative. Since the parameterized curve in the $D_2^{(\pm)}$, $D_3^{(\pm)}$, $D_4^{(\pm)}$ - space is a smooth curve, we can argue by continuity that there is an open subinterval about α_0 producing zeros of $\mathcal{P}_{4,\pm}^{(\alpha)}$ with the same property i.e. with negative real parts. Such α - values give rise to asymptotically stable equilibrium points. For α - values giving rise to curve segments located outside the first octant in the $D_2^{(\pm)}$, $D_3^{(\pm)}$, $D_4^{(\pm)}$ - space, the corresponding equilibrium points are unstable.

For the equilibrium point $Q_e^{(-)}$ given by (69), we readily find that the corresponding Routh - Hurwitz determinants $D_2^{(-)}$, $D_3^{(-)}$ and $D_4^{(-)}$ are strictly positive for the case $\alpha = 1$ i.e. $D_2^{(-)}(1) = 2.5796$, $D_3^{(-)}(1) = 1.2657$ and $D_4^{(-)}(1) = 0.1139$, which means strictly negative real part of all the zeros of $\mathcal{P}_4^{(1)}$. This result is indeed consistent with the direct computation of the eigenvalues λ_i, $i = 1, 2, 3, 4$ of the Jacobian $\mathbb{J}_4^{(1)}(Q_e^{(-)})$, as mentioned in the Section 3.3.2.

This concrete example is also consistent with the findings summarized in Fig. D.17: In this figure the α - variation of the Routh - Hurwitz determinants $D_2^{(-)}$, $D_3^{(-)}$ and $D_4^{(-)}$ for the characteristic polynomial $\mathcal{P}_{4,-}^{(\alpha)}$ corresponding to $Q_e^{(-)}$ are displayed. The input parameters used in the computations underlying these figures are given in Table 4. We observe that the Routh - Hurwitz determinants $D_2^{(-)}$, $D_3^{(-)}$ and $D_4^{(-)}$ are strictly

positive. Interestingly, $D_3^{(-)}$ depicted in Fig. D.17 is a decreasing function which approaches zero from above as $\alpha \to \alpha_-^{(2)}$. We conclude by appealing to Appendix F that the corresponding interior equilibrium point is asymptotically stable for all $\alpha \in [0, \alpha_-^{(2)})$.

In Fig. D.18 the graphs of the Routh - Hurwitz determinants $D_2^{(+)}$, $D_3^{(+)}$ and $D_4^{(+)}$ for the characteristic polynomial $\mathcal{P}_{4,+}^{(\alpha)}$ corresponding to $Q_e^{(+)}$ as functions of α on the interval $[0, \alpha_+^{(2)})$ are shown. We readily observe that $D_3^{(+)}(\alpha) < 0 < D_4^{(+)}(\alpha)$ for all $\alpha \in [0, \alpha_+^{(2)})$, which means that $Q_e^{(+)}$ is unstable for all these α - values.

We finally notice that the positive slope condition $R'(\psi_e, \gamma_{13}) > 0$ for the remediation function is fulfilled for $Q_e^{(-)}$, whereas for $Q_e^{(+)}$ we have $R'(\psi_e, \gamma_{13}) < 0$ for the concrete examples summarized in Figs. D.17 and D.18. Thus, the stability results obtained in the special cases studied in Section 3.2.3 carry over to the general case.

Appendix E

Low aquaculture production effect on the biomass growth ($0 < \alpha \ll 1$).

For the case $0 < \alpha \ll 1$, our modeling framework (20)–(23) becomes in accordance with Vasil'eva et al. (1995) a regularly perturbed system with α as a perturbation parameter:

$$\frac{d\mathbf{x}}{d\tau} = \mathbf{F}(\mathbf{x}, \alpha) = \mathbf{F}_0(\mathbf{x}) + \alpha \mathbf{F}_1(\mathbf{x}). \tag{E.1}$$

Here $\mathbf{F}_0$ and $\mathbf{F}_1$ are the vector fields

$$\mathbf{F}_0(\mathbf{x}) = (\xi \mathcal{F}_0(\mathbf{x}), \theta \mathcal{G}(\mathbf{x}), \mathcal{H}(\mathbf{x}), \mathcal{K}(\mathbf{x}))^T \quad \mathbf{F}_1(\mathbf{x}) = (-\xi\psi, 0, 0, 0)^T \tag{E.2}$$

where $\mathbf{x} = (\xi, \theta, \eta, \psi)^T$. The function $\mathcal{F}_0$ is defined as

$$\mathcal{F}_0(\mathbf{x}) = 1 - \xi - \theta$$

whereas the functions $\mathcal{G}$, $\mathcal{H}$ and $\mathcal{K}$ are given as (25)–(27), respectively.

Let us assume that $0 < \alpha \ll 1$. According to Vasil'eva et al. (1995) the asymptotic approximation of the solution of the initial value problem for (E.1) is given by the power series expansion in α i.e.

$$\mathbf{x}(\tau) = \mathbf{x}_0(\tau) + \alpha \mathbf{x}_1(\tau) + \cdots \tag{E.3}$$

in this case. Here $\mathbf{x}_0$, $\mathbf{x}_1$,... satisfy the hierarchy of initial value problems

$$\frac{d\mathbf{x}_0}{d\tau} = \mathbf{F}_0(\mathbf{x}_0), \quad \mathbf{x}_0(0) = \hat{\mathbf{x}}_0, \tag{E.4}$$

$$\frac{d\mathbf{x}_1}{d\tau} = \frac{\partial \mathbf{F}_0}{\partial \mathbf{x}}(\mathbf{x}_0)\cdot\mathbf{x}_1 + \mathbf{F}_1(\mathbf{x}_0), \quad \mathbf{x}_1(0) = \mathbf{0},$$
$$\vdots \tag{E.5}$$

where $\hat{\mathbf{x}}_0 \in \Sigma$ denotes the initial condition of the system (E.1). This means that the leading order approximation of the solution is described by means of $\mathbf{x}_0$. We also notice that the evolution of the components in the perturbation $\mathbf{x}_1$ is governed by a linear first order, nonhomogeneous system.

The outcome of the analysis of existence and stability of equilibrium points can be summarized in the following way:

1. *Existence of equilibrium points.* Assume that we have an equilibrium point $\mathbf{x}_0$ for $\alpha = 0$. This means that

   $$\mathbf{F}(\mathbf{x}_0, 0) = \mathbf{F}_0(\mathbf{x}_0) = \mathbf{0}.$$

   Then the Jacobian $\mathbb{J}_4^{(0)}$ defined by means of (D.1) is non-singular if an only if $\mathbb{J}_3^{(0)}$ defined by

   $$\mathbb{J}_3^{(0)} = \begin{pmatrix} -\xi_e & -\xi_e & 0 \\ \theta_e \frac{\partial \mathcal{G}}{\partial \xi}(Q_e^{(\pm)}) & \theta_e \frac{\partial \mathcal{G}}{\partial \theta}(Q_e^{(\pm)}) & \theta_e \frac{\partial \mathcal{G}}{\partial \eta}(Q_e^{(\pm)}) \\ \frac{\partial \mathcal{H}}{\partial \xi}(Q_e^{(\pm)}) & \frac{\partial \mathcal{H}}{\partial \theta}(Q_e^{(\pm)}) & \frac{\partial \mathcal{H}}{\partial \eta}(Q_e^{(\pm)}) \end{pmatrix} \tag{E.6}$$

   is non-singular. The vector function $\mathbf{F}$ is a smooth function of $(\mathbf{x}, \alpha)$ where $\mathbf{x} \in \Sigma$ and for all $\alpha \in \mathbb{R}$. The implicit function theorem implies that there is a unique smooth parametrization C: $\mathbf{x} = \mathbf{x}(\alpha)$; $\alpha \in [0, \varepsilon)$ for some $\varepsilon > 0$ satisfying

   $$\mathbf{F}(\mathbf{x}(\alpha), \alpha) = \mathbf{0}, \quad \mathbf{x}(0) = \mathbf{x}_0.$$

2. *Stability of equilibrium points.* Assume that $\mathbf{x}_0$ is a hyperbolic equilibrium point of the dynamical system (E.4) (which means that the real part of all the eigenvalues of $\mathbb{J}_3^{(0)}$ is non-zero). Then C: $\mathbf{x} = \mathbf{x}(\alpha)$; $\alpha \in [0, \varepsilon)$ also represents a hyperbolic equilibrium point of the system (E.1). This means that the dynamical system (E.1) is locally structurally stable about its equilibrium point for $\alpha = 0$. The stability properties in the $\alpha \neq 0$ - case emerge as a continuous deformation of the stability properties of the $\alpha = 0$ - case.

Appendix F

The Routh-Hurwitz criterion for a quartic polynomial.

The Routh-Hurwitz criterion gives necessary and sufficient conditions for all the roots of a nth degree polynomial $\mathcal{P}_n$ in λ to be located in the left-half plane (Hurwitz, 1895). In the present paper we apply this criterion in the case $n = 4$.

The starting point is the quartic polynomial

$$\mathcal{P}_4(\lambda) = \lambda^4 + a_1\lambda^3 + a_2\lambda^2 + a_3\lambda + a_4. \tag{F.1}$$

The location of the eigenvalues of this Jacobian can be determined by appealing to the Routh-Hurwitz criterion: The Routh-Hurwitz determinants D_1, D_2, D_3 and D_4 are given as

$$D_1 = a_1, \quad D_2 = a_1a_2 - a_3,$$
$$D_3 = a_1a_2a_3 - a_1^2a_4 - a_3^2, \quad D_4 = a_4D_3. \tag{F.2}$$

The Routh-Hurwitz criterion says that $D_n > 0$, $n = 1, 2, 3, 4$ and $a_4 > 0$ if and only if $Re(\lambda_n) < 0$, $n = 1, 2, 3, 4$ where λ_n, $n = 1, 2, 3, 4$ denote the zeros of $\mathcal{P}_4$, i.e., $\mathcal{P}_4(\lambda_n) = 0$.

References

Anderson, J.L., 1985. Market interactions between aquaculture and the common-property commercial fishery. Mar. Resour. Econ. 2 (1), 1–24.

Arnold, V.I., 1988. Geometrical Methods in the Theory of Ordinary Differential Equations. Springer Verlag, Boston, USA.

Bergland, H., Pedersen, P.A., Wyller, J., 2018. Stable and unstable equilibrium states in a fishery–aquaculture model. Nat. Resour. Model. e12200. https://doi.org/10.1111/nrm.12200.

Bergland, H., Pedersen, P.A., Wyller, J., 2019. Accumulated marine pollution and fishery dynamics. Ecol. Complexity 38, 56–74.

Burridge, L., Weis, J.S., Cabello, F., Pizarro, J., Bostick, K., 2010. Chemical use in salmon aquaculture: a review of current practices and possible environmental effects. Aquaculture 306 (1–4), 7–23.

Chakraborty, K., Jana, S., Kar, T., 2012. Effort dynamics of a delay-induced prey–predator system with reserve. Nonlinear Dyn. 70 (3), 1805–1829.

Christensen, P., 2017. Fish farming - a new coastal industry 1970–2015. In: Kolle, N., Nielssen, A.R., Døssland, A., Christensen, P. (Eds.), Fish, Coast and Communities. A history of Norway. Fagbokforlaget.

Cosner, C., 2014. Reaction-diffusion-advection models for the effects and evolution of dispersal. Discrete Contin. Dyn. Syst. A 34 (5), 1701–1745.

Cushing, J.M., 2013. Integrodifferential Equations and Delay Models in Population Dynamics. vol. 20 Springer Science & Business Media.

Dempster, T., Uglem, I., Sanchez-Jerez, P., Fernandez-Jover, D., Bayle-Sempere, J., Nilsen, R., Bjørn, P.A., 2009. Coastal salmon farms attract large and persistent aggregations of wild fish: an ecosystem effect. Mar. Ecol. Prog. Ser. 385, 1–14.

Flaaten, O., 2018. Fisheries Economics and Management, second ed. Ola Flaaten and bookboon.com.

Foley, N.S., Armstrong, C.W., Kahui, V., Mikkelsen, E., Reithe, S., 2012. A review of bioeconomic modelling of habitat-fisheries interactions. Int. J. Ecol. 2012, 1–11.

Ghosh, B., Kar, T., 2014. Sustainable use of prey species in a prey–predator system: jointly determined ecological thresholds and economic trade-offs. Ecol. Modell. 272, 49–58.

Golden, J., Virdin, J., Nowacek, D., Halpin, P., Bennear, L., Patil, P., 2017. Making sure the blue economy is green. Nat. Ecol. Evol. 1 (17). https://doi.org/10.1038/s41559-016-0017.

Gordon, H.S., 1954. The economic theory of a common-property resource: the fishery. Classic Papers in Natural Resource Economics. Springer, pp. 178–203.

Gravelle, H., Rees, R., 2004. Microeconomics, third ed. Prentice Hall, London, England.

Grefsrud, E., Glover, K., Grøsvik, B., Husa, V., Karlsen, Ø., Kristiansen, T., Kvamme, B., Mortensen, S., Samuelsen, O., Stien, L., Svåsand, T., 2018. Risk Assessment of Norwegian Fish Farming. 2018 (Risikorapport norsk fiskeoppdrett 2018). Institute of Marine Research. (In Norwegian)

Guckenheimer, J., Holmes, P., 1983. Nonlinear Oscillations, Dynamical Systems, and Bifurcations of Vector Fields. Springer-Verlag, New York, USA.

Haavelmo, T., 1971. The pollution problem from social science point of view (forurensingsproblemet fra samfunnsvitenskapelig synspunkt). Sosialøkonomen (4), 5–8. (In Norwegian)

Hannesson, R., 1983. Optimal harvesting of ecologically interdependent fish species. J. Environ. Econ. Manage. 10 (4), 329–345.

Hannesson, R., 2003. Aquaculture and fisheries. Mar. Policy 27 (2), 169–178.

Heilmann, I.T., Thygesen, U.H., Sørensen, M.P., 2018. Spatio-temporal pattern formation in predator-prey systems with fitness taxis. Ecol. Complexity 34, 44–57.

Hersoug, B., 2012. The fight for space on the coast - a historical sketch(kampen om plass på kysten - en historisk skisse). In: Hersoug, B., Johnsen, J.P. (Eds.), The fight for space on the coast(Kampen om plass på kysten. Interesser og utviklingstrekk i kystsoneplanleggingen). Universitetsforlaget. (In Norwegian)

Hoagland, P., Jin, D., Kite-Powell, H., 2003. The optimal allocation of ocean space: aquaculture and wild-harvest fisheries. Mar. Resour. Econ. 18 (2), 129–147.

Hurwitz, A., 1895. Ueber die bedingungen, unter welchen eine gleichung nur wurzeln mit negativen reellen theilen besitzt. Math. Ann. 46 (2), 273–284.

Jiang, S., 2010. Aquaculture, capture fisheries, and wild fish stocks. Resour. Energy Econ. 32 (1), 65–77.

Kathijotes, N., 2013. Keynote: Blue economy-environmental and behavioural aspects towards sustainable coastal development. Procedia-Social Behav. Sci. 101, 7–13.

Liu, Y., Olaussen, J.O., Skonhoft, A., 2014. Fishy fish? The economic impacts of escaped farmed fish. Aquacult. Econ. Manage. 18 (3), 273–302.

Logan, J.D., 1987. Applied Mathematics: A Contemporary Approach, New York: J. New York, NY (USA); John Wiley and Sons Inc.

Lorenzen, K., Beveridge, M., Mangel, M., 2012. Cultured fish: integrative biology and management of domestication and interactions with wild fish. Biol. Rev. 87 (3), 639–660.

Mikkelsen, E., 2007. Aquaculture-fisheries interactions. Mar. Resour. Econ. 22 (3), 287–303.

Murray, J.D., 2001. Mathematical Biology. II Spatial Models and Biomedical Applications {Interdisciplinary Applied Mathematics V. 18}. Springer-Verlag New York Incorporated.

NFD, 2014. Forutsigbar og miljømessig bŌrekraftig vekst i norsk lakse og ørretoppdrett. stortingsmelding 16 (2014-2015).Forutsigbar og miljømessig bŌrekraftig vekst i norsk lakse og ørretoppdrett. stortingsmelding 16 (2014-2015).

Øksendal, B., 2003. Stochastic Differential Equations. Springer-Verlag Berlin Heidelberg. Springer-Verlag, Berlin Heidelberg.

Perko, L., 2013. Differential Equations and Dynamical Systems. vol. 7 Springer Science & Business Media.

Regnier, E., Schubert, K., 2016. To what extent is aquaculture socially beneficial? A theoretical analysis. Am. J. Agric. Econ. 99 (1), 186–206.

Schaefer, M.B., 1954. Some aspects of the dynamics of populations important to the management of the commercial marine fisheries. Inter-Am. Trop. Tuna Comm. Bull. 1 (2), 23–56.

Silver, J.J., Gray, N.J., Campbell, L.M., Fairbanks, L.W., Gruby, R.L., 2015. Blue economy and competing discourses in international oceans governance. J. Environ. Dev. 24 (2), 135–160.

Smith, V.L., 1969. On models of commercial fishing. J. Polit. Economy 77 (2), 181–198.

Smith-Godfrey, S., 2016. Defining the blue economy. Marit. Aff. 12 (1), 58–64.

Spalding, M.J., 2016. The new blue economy: the future of sustainability. J. Ocean Coastal Econ. 2 (2), 8.

Steinshamn, S.I., 2017. Predators in the market: implications of market interaction on optimal resource management. J. Bioecon. 19 (3), 327–341.

Svåsand, T., Kvamme, B.O., Stien, L.H., Taranger, G.L., Boxaspen, K.K., 2016. Risk Assessment of Norwegian Fish Farming. 2016 (Risikovurdering av norsk fiskeoppdrett. 2016. Institute of Marine Research. (In Norwegian)

Vasil'eva, A.B., Butuzov, V.F., Kalachev, L.V., 1995. The Boundary Function Method for Singular Perturbation Problems. vol. 14 Siam.

Watson, S.C., Paterson, D.M., Queirós, A.M., Rees, A.P., Stephens, N., Widdicombe, S., Beaumont, N.J., 2016. A conceptual framework for assessing the ecosystem service of waste remediation: in the marine environment. Ecosyst. Serv. 20, 69–81.